Title:

Analysis and Modeling of Sea-Level Variability in the Chesapeake Bay using the Regional Ocean Modeling System (ROMS)

Brittany L. Bruder
Department of Civil and Environmental Engineering
Georgia Institute of Technology, Savannah Campus

John R. Moisan*
Laboratory for Hydrospheric and Biospheric Sciences
NASA Goddard Space Flight Center
Wallops Island, VA 23337

Jiangtao Xu
National Oceanic and Atmospheric Administration
National Ocean Service
Climate Survey Development Laboratory
1315 East-West Highway
Silver Spring, MD 20910
&
Michael F. Jasinski
Laboratory for Hydropsheric and Biospheric Sciences
NASA Goddard Space Flight Center
Greenbelt, MD 20771

1 September, 2010

*Corresponding author: John.R.Moisan@nasa.gov

Abstract

Sea level height variability in the Chesapeake Bay for 2006 is analyzed using a three-dimensional, regional circulation model (Regional Ocean Modeling System: ROMS) in order to understand the spatial and temporal scales of this variability in the context of the various phenomena such as tides and forcing fields such as wind, evaporation-minus-precipitation, and river fluxes. Standard harmonic analysis is applied to hourly simulations of the model's free surface to obtain the amplitude and phase of 39 tidal components at each model grid location within the bay. The resulting tidal components are removed from the full free surface time series to obtain time series of the subtidal 'residuals'. Empirical Orthogonal Function (EOF) analysis is carried out on these 'residuals,' and the first EOF accounts for 91.2% of the observed variance. The corresponding time series from this first EOF is highly correlated to the northwest-southeast component of the mean wind field, and demonstrates the influence of the larger scale, longer term impact of winds on retarding or enhancing flow of water through the bay mouth. The second EOF component accounts for an additional 6.6% of the observed variance of the residuals. The corresponding time series from this second EOF demonstrates the influence of the local north-south wind field component in developing a north/south-oriented seiche mode within the Bay. Precipitation, evaporation and fluvial fluxes have minimal influence on the bay's sea level variability. The influence fluvial fluxes are limited to the headwaters of the bay and account for a small amount of the overall sea level variability. The east-west component of the local wind field appears to have a more important influence in the Bay's headwater regions, where westward wind components correlate to lower sea-levels.

Introduction

Understanding the processes that control both the short-term (tides and storms) and long-term (climate and climate change processes) sea-level variability in the coastal ocean and bays is important to a wide range of human related activities, such as fishing, shipping, recreation, transportation, agriculture, and necessary for correct prediction of flooding potentials in low lying coastal areas. Short-term sea level variability in coastal regions is influenced primarily by tides that, while forced through gravitational forcing from various astronomical bodies, are primarily altered in coastal areas as a result of the bathymetry and morphology of the coastal region. Winds and freshwater fluxes (primarily river inputs) also impact sea level variability. The level to which various physical processes influence sea level variability depends on the time-scales of interest, ranging from the shorter periods associated with processes linked to tidal and gravity wave speeds to much longer climate-related processes, such as changes in mean wind and precipitation patterns.

The Chesapeake Bay is the largest embayment is the U.S. The

For instance Barbos and Silva (2009) used long tide gauge records to point out that long-term sea-level variability in the Chesapeake Bay is influenced at the annual scale primarily by atmospheric pressure and zonal wind but at longer time scales the precipitation rate, which alters both fluvial inputs and the overall dynamic height of the bay through modulation of the salinity field, is the key driver.

The U. S. National Aeronautics and Space Administration (NASA) is presently developing the Surface Water Ocean Topography (SWOT) mission, an interdisciplinary mission

aimed at observing water levels in rivers, lakes and wetlands as well as sea-levels in both the open and coastal ocean regions. Such a new topographic capability for the coastal ocean can be of great benefit in providing answers to a host of scientific questions related to how land processes influence coastal oceans and bays. In developing the technical requirements for such a mission it becomes necessary to develop a greater understanding of the spatial and temporal scales of variability that various physical processes have on the coastal ocean sea-level.

The variability of the Bay's sea-level has been the topic of numerous studies. Tidal Wang and Elliot (1978) noted that subtidal sea-level fluctuations were induced non-locally by coastal winds that drove water into (out of) the Bay during periods of southward (northward) winds through a coastal Ekman effect.

Bosley and Hess (2001), using hourly wind observations from 1994, show that coherence between subtidal sea-level at Baltimore and wind stress Thomas Point Light (a NOAA weather station located just north of the Chesapeake Bay Bridge) shows consistently significant (0.6—0.8) levels for all periods of wind forcing. EOF analysis on six years (1991-1996) of hourly sea-level measurements (30 hour low-pass filtered) from 10 NOAA National Ocean Service water level gauges and wind observations from the NOAA National Data Buoy Center (NDBC) CBBT buoy revealed that the first two modes accounted for 97-99% of the observed variability. The first mode accounted for most of the signal and showed uniform amplitude over the entire bay, demonstrating a constant rise and fall of the bay that is neither amplified nor attenuated over different portions of the bay. It is a clear demonstration of the influence of the coastally driven variability on the bay itself. The second mode was tilted with a nodal line located between

Gloucester Point and Lewisetta. This mode accounted for only 15.8% of the variability and is thought to result from direct local wind forcing over the bay.

The seasaw-like variability observed in the second EOF has been characterized by Chuang and Boicourt (1989) as a resonant seiche mode driven by the longitudinal north-south wind at 2-3 day time scales.

Gong and Shen (2009), in a 3D numerical study that investigated the influence of northeaster storms on the Chesapeake Bay, show that the relative importance of the local and remote winds in generating storm surges in the Bay varied with different northeasters.

The impact of larger scale wind forcing events, such as from hurricanes, can also influence sea levels within the Bay. Li et al. (2006) used the ROMS model to investigate the impact of the 2003 hurricane Isabel storm. The eye of the storm passed inland to the south of the Bay and the wind across the Bay were strong south-to-southeast, blowing the water into the northern head of the Bay. Such an event, argue Li et al. (2006) may set up a seiche resonance, an event that was previously observed in the Bay by Chuang and Boicourt (1989) for specific north-south wind events and argued by Boicourt (2005) to have occurred during passage of hurricane Isabel.

Li et al. (2005) initially configured the ROMS model and demonstrated its ability to simulate tidal sea level variability in addition to the 3D circulation patterns from baroclinic and barotropic processes.

A similar influence of the northwest wind on sea-level variations in the Chesapeake Bay during the 1999 Hurricane Floyd has been shown in a 2D barotropic model simulation by Shen and Gong (2006). The results from this study also note, however, that the storm tide also had a significant impact.

Shen, J., H. Wang, et al. (2006). "Storm tide simulation in the Chesapeake Bay using an unstructured grid model." Estuarine Coastal and Shelf Science 68(1-2): 1-16.

Hurricane Isabel made landfall near Drum Inlet, North Carolina on September 18, 2003 (UTC 17:00). Although it was classified as only a Category 2 storm (Saffir-Simpson scale), Hurricane Isabel had a significant impact on the Chesapeake Bay with a 1.5-2.0 m storm surge (above mean sea level), and was dubbed the "100-year storm". A high-resolution unstructured grid model (UnTRIM) was applied to simulate storm tide in the Chesapeake Bay. The application of an unstructured grid in the Bay offers the greatest flexibilities in representing complex estuarine geometry near the coast and encompassing a large modeling domain necessary for storm surge simulation. The resulting mesh has a total of 239,541 surface elements. The model was forced by 9 tidal harmonic constituents at the open boundary and a wind field generated by a parametric wind model. A hindcast simulation of Hurricane Isabel captures both peak storm tide and surge evolution in various sites of the Bay. Model diagnostic studies indicate that the high surge occurring in the upper Bay regions was mainly caused by the forced southerly

wind, whereas the offshore surge and both the northeasterly and southeasterly winds influenced the lower Bay region more significantly. (c) 2006 Elsevier Ltd. All tights reserved.

Valle-Levinson, A., C. Reyes, et al. (2003). "Effects of bathymetry, friction, and rotation on estuary-ocean exchange." Journal of Physical Oceanography 33(11): 2375-2393.

An analytical model that includes pressure gradient, friction, and the earth's rotation in both components of the flow is used to study the transverse structure of estuarine exchange flows and the nature of transverse circulation in estuaries of arbitrary bathymetry. Analytical results are obtained for generic bathymetry and also over real depth distributions and are compared with observations. This study extends previous efforts on the topic of transverse structure of density-induced exchange flows in three main aspects: 1) the analytical model explores any arbitrary bathymetry; 2) the results reflect transverse asymmetries, relative to a midchannel centerline, associated with the effects of the earth's rotation; and 3) the transverse circulation produced by the analytical model is examined in detail. Analytical results over generic bathymetry show, in addition to the already reported dependence of exchange flow structure on the Ekman number, two new features. First, the transverse structure of along-estuary flows shows the earth's rotation effects, even in relatively narrow systems, thus producing transverse asymmetries in these flows. The asymmetries disappear under strongly frictional (high Ekman number) conditions, thus illustrating the previously documented pattern of inflow in channels and outflows over shoals for typical estuaries. Second, transverse flows resemble a "sideways gravitational circulation" when

frictional effects are apparent (Ekman number greater than similar to0.1) responding to a transverse balance between pressure gradient and friction. These transverse flows reverse direction under very weak friction and reflect Coriolis deflection of along-estuary flows, that is, geostrophic dynamics. All examples of observed flows are satisfactorily explained by the dynamics included in the analytical model.

Valle-Levinson et al. (2001)

Water density and velocity data from two similar to 75-day deployments across the entrance to the Chesapeake Bay were used in conjunction with wind velocity and sea level records to describe the transverse structure of wind-induced subtidal exchange. Acoustic Doppler current profilers, electromagnetic current meters, and conductivity-temperature-depth recorders were deployed at the entrance to the bay from mid-April to early July of 1999 and from early September to mid-November of 1999. Three main scenarios of wind-induced exchange were identified: (1) Northeasterly (NE) winds consistently drove water from the coast toward the lower Chesapeake Bay as well as water from the upper bay to the lower bay, which was indicated by the surface elevation slopes across the lower bay and along the bay, This resulted in water piling up against the southwestern corner of the bay. The subtidal flow over the southern portion of the bay entrance was directed to the left of the wind direction, likely the result of the influence of Coriolis and centripetal accelerations on the adjustment of the sea level gradients, Over the northern shallow half of the entrance, the subtidal flows were nearly depth-independent and in the same direction as the wind. (2) Southwesterly (SW) winds caused opposite sea level gradients (relative to NE winds), which translated into near-surface outflows throughout the entrance and near-bottom inflows restricted to the channels. This wind-induced circulation

enhanced the two-way exchange between the estuary and the adjacent ocean. (3) Northwesterly winds produced the same exchange pattern as NE winds. Water piled up against the southwestern corner of the bay causing net outflow in the deep, southern area and downwind flow over the shallow areas. Northwesterly winds greater than 12 m/s caused the most efficient flushing of the bay, driving water out over the entire mouth of the estuary.

Wang, D. P. (1979)

Wang, D. P. and A. J. Elliott (1978) found that short-term sub-tidal sea-level variability at frequencies of 2-4 day correlated well with the local along-eastuary (N/S???) winds, while longer

Similar conclusions were also obtained for the Delaware Bay by Wong and Moses-Hall (1998) using sea level and current measurements to demonstrate that the remote wind effect, through impingement on the coastal sea level at the mouth of the estuary, had more influence on the subtidal sea level fluctuations in the interior of the bay but that local winds were more important in producing spatial variability in the circulation within the bay.

Using observations of horizontal velocity from Acoustic Doppler Current Profilers (ADCP) and electromagnetic current meters deployed at six separate locations across the bay entrance in conjunction with wind velocity and sea level records, Wong and Valle-Levinson (2002) demonstrated that at subtidal time scales the net flux integrated over the entrance to the estuary adequately describes the unidirectional (either inflow or outflow over the entire cross-section) barotropic volume flux associated with the coastally forced remote wind effect.

In a modeling study Zhong et al. (2008) demonstrated that the Chesapeake Bay is highly dissipative, yielding a relatively lower resonant responses due to a much larger bottom friction than other coastal areas.

Phenomenon of the Tides

Due to the patterned consistency of these astrological movements, the motion of the tide proper and water level for a given location can be represented kinematically through a sum of harmonic expressions (INSERT EQUATION). Each harmonic constituent represents the rise and fall of surface height caused by one of the n astrological forcings of the tide. The corresponding angular frequencies, ω_n, are known characteristics based on planetary motions and are constant in time and space. The coefficients, h_n, known as harmonic constants, as well as the phase displacements, α_n, are constant in time but vary with location.

This set of unique harmonic constants and phase displacements can be assessed for a given location by an analysis of local water levels recorded at a high temporal resolution over an extended period of time (1 sample/hr and 12 months, respectively). This computational process, known as harmonic analysis, can be used to predict surface heights at a given location and time. Such predictions of the ocean tide can be used for coastal construction, commercial and recreational marine activities, environmental and biological transport, beach erosion, and feasibility studies of tidal-electric energy projects (Bosley and Hess 2001).

Sub-Tidal Modifications in Estuaries and the Chesapeake Bay

Concerning harmonic analysis, the duality of the tidal forcings in the Chesapeake produces a variation in harmonic constituents and phase displacements across the bay (Li, Zhong et al. 2006; Zhong, Li et al. 2008). The tide in the southern portion of the bay is considered semidiurnal: the composition of the sum of its harmonics is dominated by M_2, S_2, and N_2,[1] all forcings with an angular frequency of approximately two cycles per solar day. The central and northern parts of the bay are considered to have a mixed tide; two tidal cycles occur per solar day, however the tidal range of each cycle also oscillates with a period of one solar day. Its harmonic sum is a dominated by both semidiurnal and diurnal forcings; in addition to the semidiurnal components, the diurnal forcings K_2 and O_2,[2] also have large coefficients (Li, Zhong et al. 2006). It is not this variation in harmonics across the bay that limits the effectiveness of harmonic analysis in Chesapeake tidal prediction, but rather additional non-periodic forcings outside astrology found locally throughout the bay.

Although harmonic analysis can be effective in predicting tides along ocean shores, it only serves as a basis for tidal predictions in coastal estuaries and bays such as the Chesapeake. Once a tidal stream has entered a bay, local forcings, characterized as 'sub-tidal', modify the original parameters of the ocean tide resulting in a deviation of surface heights from harmonic predictions (Valle-Levinson, Wong et al. 2001). The three most prominent characterizations of sub-tidal forcings in bays and estuaries defined by Albert Defant in his book Ebb and Flow, 1958, are:

Resonance: The bathymetry and geography of the estuary dictate the natural resonant frequency of the locale. If similar to the frequency of the tide, oscillations in the tide will occur, resulting in much greater tidal ranges. Typically, this resonant frequency is constant on a geological time scale; its effects on the tide are consistent and can be planned for. However, marine construction such as a barrage can alter the natural frequency of the estuary or bay and further change the original tidal parameters and predictions.

Freshwater Inflow: Freshwater runoff from rivers can increase the surrounding water levels in the bay or estuary. The shear volume of inflow can alter the local surface heights as well as the circulation induced by the salinity gradient cause by the exchange of fresh and salt water. Nominal inflows and their effects can be predicted and planned for; however strong storm events can flood rivers, making their fluxes and effects on surface heights more difficult to predict.

Wind Events: Along with a corresponding change in barometric pressure, wind events, both long and short term, can drive coastal waters away or towards the shore. Coupled with a peak high tide, tidal surges can occur resulting in extreme damage and erosion. While seasonally meteorological patterns can be discerned for extended periods of time, isolated wind events are far less consistent. The magnitude and direction of winds can be highly variable in space and time, muddling their effects across the bay and making tidal prediction difficult.

These sub-tidal forcings are far less consistent than the planetary movements considered in harmonic analysis, making the prediction of estuarine water levels far more complex. The Chesapeake Bay is particularly susceptible to sub-tidal forcings, making water levels notoriously difficult to predict. Properties of the bay that enable sub-tidal susceptibility are the shallow bathymetry, weak tidal currents, and multiple inflows from tributaries (Valle-Levinson, Reyes et al. 2003). Both the local urban and natural environments rely heavily on the physical oceanographic processes of the Chesapeake and are vulnerable to any abnormalities in its behavior. Sub-tidal deviations from tidal predictions in the Chesapeake Bay are not only significant in magnitude but also significant in environmental impact.

1.3 Previous Sub-Tidal Exploration in the Chesapeake Bay

As a result of the high variability and environmental impact of water levels, much research has been conducted to better predict and understand the local sub-tidal components of the tide and their effects in the Chesapeake Bay. The perceived physical processes in the bay have evolved alongside the progression of spatial and temporal resolution in the observational data in the past 60 years.

In the 1950s and 1960s, much of the sub-tidal variation was thought to be caused by gravitational circulation (Wang and Elliott 1978). It was not until the 1970s that a focus on meteorological events and resonant oscillations began surfacing in research alongside continuous current measurements. In 1978, Wang and Elliot studied sea levels and meteorological records at seven points in the Chesapeake for two months along with near bottom current measurements at the Potomac River. Using harmonic analysis, they pulled the tidal variations from the observed sea

level data and determined the spatial distributions of the sub-tidal variations through an empirical orthogonal function analysis (EOF analysis).

The first mode resulting from the EOF analysis accounted for 90% of the total variance and showed coherent fluctuations across the bay. From the first mode, it was found that low frequency fluctuations at the mouth of the bay propagated up towards the head. This non-local forcing controlled the majority of the sea level variation in the Chesapeake. Higher frequency variations at the head of the bay, in constant phase with the mouth fluctuations, were assumed to be the result of resonant oscillations from the mouth.

Cross correlation analysis performed on the principle component of the primary EOF and wind speeds suggested a high correspondence with mouth fluctuations with cross and along shore winds. It was assumed crosswinds created a direct flux of coastal waters while along shore winds induced an Ekman push. Individual cross correlations performed on site water levels and wind showed a high correlation with local winds at high frequencies. Ultimately it was asserted that two time scales existed for sub-tidal forcings: long term and large scale fluctuations originating at the bay mouth and local short term fluctuations due to meteorological events.

Wang and Elliot ( ) acknowledged that in order for their assertions to be verified and to further the study of sub-tidal forcings in the Chesapeake, three steps needed to be taken: procure longer time series of observational data to observe seasonal and storm events; have a higher spatial resolution in observational data to observe non-local fluctuations across the bay; and expand the data domain to include wind and water levels of surrounding coastal waters. These final

posturings have only begun to be successfully tackled in the past ten years. With advancement of spatial and temporal resolution in data observation techniques, many of the uncertainties and questions posed by Elliot and Wang's research have been answered.

In the spring and fall of 1999, Valle-Levison, Wong, and Bosely were able further elaborate on the fluctuations found at the bottom of the bay by operating six moorings stationed across the mouth for two 75 day deployments in conjunction with point surface height measurements at NOAA stations across bay. In addition to recording local wind and surface heights, the moorings were equipped with acoustic Doppler current profilers to provide current measurements resolutely across the entire water column.

This intensified study of the coastal water exchange ultimately disproved Wang and Elliot's assertion of an Ekman push. However, Wang and Elliot's theory that bay fluctuations were forced by wind driven fluctuations at the mouth withstood the scrutiny of the new techniques and was verified by Valle-Levison, et al. Wang and Elliot's spatial distribution of fluctuations from the EOF analysis was also verified through qualitative analysis of point surface heights across the bay over an extended period of a few months. However, due to the scope of the project, the data had sparse spatial resolution in the head of the bay and the Valle-Levison research did not specifically address local or resonant fluctuations in the upper reaches of the Chesapeake.

In 2008, Zhong, et al, utilized observed data from NOAA stations across the Chesapeake to generate a numerical simulation of the physical oceanography of the bay. Utilizing the regional ocean modeling system (ROMS), Zhong was able to obtain simulated observational data at a high temporal and spatial resolution. With access to wide-spread current profile, wind, and

surface height data, Zhong was able to conclude that resonant oscillations have limited effect on surface heights due to the high dissipation of energy in the shallow Chesapeake Bay. Contrary to Want and Elliot, Zhong suggested such oscillation in the head of the bay was wind driven, but not a resonant oscillation in response to the wind.

It can be seen through this historical catalog of research that in order to gain a complete understanding of the physical oceanographic processes in the Chesapeake Bay, observed data must be highly resolute in time and space due to the frequent variation of water levels locally across the bay. This study will show, even when employing the same successful EOF and cross correlation analysis method as Wang and Elliot ( ), a data set with higher temporal and spatial resolution can produce differing and more comprehensive results furthering progress towards an effective method of tidal prediction in the Chesapeake Bay.

Methods

Circulation Model and Obtained Data

A four-dimentional (time and space) ocean circulation model is applied to simulate the tidal and sub-tidal circulation dynamics of the Chesapeake Bay during the period of 2006. This "ChesROMS" model (Xu et al., 2010) is an open source Chesapeake Bay implementation of the Regional Ocean Modeling System (ROMS; Shchepetkin and McWilliams, 2005). ROMS is a free surface, terrain-following, primitive equations ocean model with several coupled models for biogeochmical, sediment and sea ice applications. The hydrodynamic model solves the primitive equations on horizontally orthogonal curvilinear grids and vertically terrain-following sigma coordinates with time integration split into external mode and internal mode for momentum. ChesROMS has a 150x100 horizontal grid with 20 levels in the vertical. Figure 1 shows the model grid with bathymetry for this implementation. ChesROMS is forced by open-ocean tides,

river discharge, winds and heat exchange across the air-water surface. At the open-ocean boundary the model is forced using nine tidal constituents from the Advanced Circulation Model (ADCIRC) EC2001 tidal database (Mukai et al, 2002), together with non-tidal water levels interpolated from the National Oceanic and Atmospheric Administration's (NOAA) tide stations at Wachapreague, Virginia and Duck, North Carolina. Chapman's condition for surface elevation (Chapman, 1985) and Flather's condition for barotropic velocity (Flather, 1976) were applied to the barotropic component at the open-ocean boundary, while for the baroclinic component a radiation condition was used for velocity and a radiation condition with nudging for temperature and salinity. Daily freshwater discharge data for nine major tributaries (Susquehanna, Patuxent, Potomac, Rappahannock, York, James, Nanticoke, Choptank and Chester Rivers) from USGS were applied at the upstream river boundaries. At the open-ocean boundary, climatological temperature and salinity are specified using data from the World Ocean Atlas (WOA) 2001. Atmospheric forcing, including 3-hourly winds, net shortwave and downward longwave radiation, air temperature, relative humidity and pressure were obtained from the North America Regional Reanalysis (NARR). The physical model had been run for 15 years from 1991 to 2005 and validated against available observations of water level, temperature, salinity and velocity (Xu et al., 2010). In this study, we extended the model run to 2006 in order to compare the results against better observational data from the NASA ICESAT laser altimeter.

Chesapeake Bay Sea-Level Simulation, Observations and Analysis

The sea-level variability within the Chesapeake Bay is analyzed using 8760 hourly free-surface calculations for each of the model's horizontal grid points within the Chesapeake Bay from the 2006 simulation. Model grid points outside of the Chesapeake Bay are not included in the analysis in order to remain distant from possible artifacts in the time series adjacent to open-

ocean boundaries and to maintain focus on the Chesapeake Bay itself. The free-surface time series are each subjected to harmonic analysis to compute the tidal harmonics. Subtidal sea-level heights are computed by subtracting the tidal harmonics from the raw free-surface sea-level predictions. The subtidal sea-level time series are further decomposed using a standard application of Empirical Orthogonal Function (EOF; Preisendorfer, 1988) analysis. The resulting modes of variability are compared against various model forcing fields in order to understand what physical factors control the subtidal sea-level variability within the Bay.

Field observations of surface winds and sea-level for ## locations within the Bay from the U.S. National Oceanic and Atmospheric Administration (NOAA) tide station data are used to validate model solutions and compare with the EOF analysis of the model solutions.

Harmonic Analysis of Chesapeake Bay Tides

The Harmonic Analysis by Method of Least Squares (HAMELS) is used on the simulated hourly free surface sea-level heights from the ChesROMS 2006 solution set for the Bay. While only 9 tidal harmonics (O_1, K_1, Q_1, M_1, S_2, N_2, and K_2) are used in development of the model's forcing fields (), the full set of 37 tidal components (Table 1) systematically used by NOAA to model tides () is used in the HAMELS approach

HAMELS (Harmonic Analysis by Method of Least Squares) was then performed on each time series to ascertain the unique harmonic constants, phase displacements, and resulting sum of harmonic constituents for each point. Provided a set of specified celestial angular frequencies, HAMELS utilizes the least squared criterion to find the corresponding harmonic constituent coefficients and phase displacements that will produce the minimal possible sum of the squared differences between the surface height time series and the sum of harmonic

constituents. (INSERT EQUATION) In this study 39 harmonic constituents (n=39) were specified to reconstruct the tide.

For every point HAMELS produced a time series of predicted surface heights induced by the ocean tide. These time series were removed from the original ROMS surface height output resulting in a time series of residual sub-tidal surface heights for every point.

2.3 Wind Preprocessing

To analyze the correlation between the wind and the sub-tidal residual surface heights, two time series of wind magnitudes, sampled every three hours, were pulled from the ROMs output. Each time series represented the magnitude of the winds' orthogonal components specified along the xi and Etta axes of the ROMS grid. Each wind vector was then transformed into orthogonal components in the direction of East and North. Because a spherical curvilinear grid, no geographical mapping was involved and this change of basis calculation was simplified to a set of trigonometric functions for each grid point.

A calculation of wind variance across the gird for each point in time showed spatial consistency in wind magnitudes for both East and North components. To simplify analysis, the magnitudes of the two components were separately averaged across the entire grid to form two time series representing the spatially averaged North and East orthogonal components of the wind.

Although the reducing the thousands of wind time series to two greatly simplified the analysis, the directionality and vector notation of the wind data still was a challenge. The wind data was

defined in three dimensions (time, magnitude, and direction) where as the residual surface heights were defined in two (magnitude, time). In order to successfully determine the correlation of the two, the wind data had to be reduced to two dimensions (magnitude + time) while still retaining its directional identity. To do this, a change of basis was performed on the E + N time series 360 times, rotating the two orthogonal unit vectors one degree each time until a full revolution was made.

This resulted in 2 orthogonal sets of 360 time series, each series representing the magnitude of the component of the wind in that direction (the degree rotated from the original axis). With each unit vector having both positive and negative magnitudes, only the first 180 time series were required for full definition. A linear interpolation between measurements was conducted for each wind time series to increase the sampling rate of the wind data to match that of the surface height residuals (1 sample/hr). The 180 time series were analyzed with the residual heights separately, with each result being compared to find the wind direction with the highest correlation.

2.4 EOF/Cross Correlation Analysis

Because the wind forcing was initiated three days before the sampling of surface heights and ended three days after the termination of surface height sampling, a cross correlation analysis was ideal to determine the optimum time lag between the wind values and their effects on the surface heights. Cross correlation analysis measures the similarity of two time series as a function of a time lag applied to one of them. In this analysis, the time lag was applied to the wind time series.

For a selected number of data points across the bay a cross correlation analysis was performed between the residual surface height time series and each of 180 wind time series. The correlation coefficients were then plotted in three dimensions as a function of time lag and wind direction for each selected point.

Rather than compare the wind to the behavior at a point, an Empirical Orthogonal Function (EOF) analysis was performed to observe the behavior of the entire bay similar to Elliot and Wang. The time series of coefficients associated with each EOF, or spatial pattern of the bay was then analyzed against the wind in the cross correlation process mentioned above.

Results and Discussion

3.1 High Correlation Between Winds and Residual Surface Heights

Through the cross correlation analysis of the residual surface heights and all wind directions, it was found that the sub-tidal forcing of the wind has a significant correlation with the wind. Further correlation analysis with the EOF as seen below, shows the wind induces 97% of the sub-tidal variation. All point residuals and EOF cross correlations showed a maximum

correlation coefficient of approximately .75 with the wind time series. In addition to providing the degree of correlation, the cross correlation diagrams also explicitly explained spatial and temporal relationships between the wind sub-tidal forcings and their effects of the surface height.

3.2 Interpretation of Cross Correlation Diagrams

The cross correlation diagrams proved to be a resourceful tool when analyzing wind and surface height data; each plot held substantive information about the surface height responses to wind as a function of location, wind direction, and response time. Such depth of information requires a brief explanation of the interpretation of the diagram.

Areas of high positive correlation represent a symmetric relationship between winds pointing in that in that direction and surface height, i.e. winds in that direction cause positive residuals and winds opposite of that vector (negative magnitude) cause residual surface heights below predicted values. It is imperative to note when reading this diagram that an area of high correlation for a given direction does not infer that that direction of wind has a high correlation. What it does infer is that winds along that axis, or winds in both the negative and positive direction have a high correlation with the time series. From the cross correlation diagram alone, one cannot tell which wind direction, positive or negative, on the axis is the dominant pattern. However, by use of the wind angle histogram, one can make an assumption as seen further.

A ‘slanted’ or skewed area of high correlation suggests that wind direction and the temporal timeframe of the sea surface height response are not independent. High correlations at the bottom of the area represent extended temporal responses to the winds in the corresponding direction, where high correlations at the top represent immediate responses to the winds in different

directions. When skewed areas of high positive and negative correlation overlap a given wind direction as see in line A, this signifies that the wind direction has both a negative and positive effect on surface heights in different timescales.

By the use of these cross correlation diagrams at points across the bay and in conjuncture with EOF analysis, the analysis was able to isolate both temporal and spatial patterns of surface height response to wind sub-tidal forcing.

3.3 Correlation Between Point Residuals and Winds

When analyzing the set of cross correlation diagrams for points across the Chesapeake, it was imperative to recognize wide spread similarities to find evidence of non-local wind forcing and differences to extract local forcing effects.

Similarities Across the Bay:

Diagrams below a lag time of -24 hours are almost identical across the bay: a high positive correlation at approximately 160 degrees, the direction of the mouth of the bay, and a weaker negative correlation around 270 degrees, the north/south axis. This signifies that water levels across the Chesapeake respond to fluctuations at the mouth of the bay, independent of geographical location. This non-local forcing floods or drains the entire bay uniformly over an extended period of time as it propagates northward.

Differences Across the Bay:

Unlike the long-term responses, the immediate surface height correlations (lag times above -24 hours) vary across the bay, representing evidence of local effects. At the mouth of the bay, short-term correlations are relatively unchanged compared to the long term correlations. This suggests that wind events in the direction of the mouth of the bay cause an immediate coastal water exchange that only affects the bottom of the bay. Water levels at the mouth of the bay are dominated by this coastal water exchange and no other activity.

At the northern half of the bay, short term effects differ from long term effects more drastically. The short term effects of the winds on water levels in the head of the bay are driven by a different mechanism depending on their geographic location. In all northern diagrams, a high short term correlation exists from 160-225, the direction of the head of the bay. This suggests a coastal exchange occurs at the head from the Delaware Bay, forced by wind; water levels in the head of the bay respond locally and quickly to winds in the direction of the head. Because the short term effects do not match the long term effects, it can be assumed that over a period of time, the coastal exchange at the mouth is the dominant forcing. The coastal exchange at the head, is a secondary forcing with only immediate, and local results.

The assemblage and analysis of the point cross correlation diagrams asserts that the dominant wind forcing is the coastal water exchange at the mouth of the bay, supporting the claim made by Elliot and Wang. More specifically our more resolute observation data explained additional sub tidal effects by the wind. The secondary forcing is the coastal water exchange at the head of the bay, induced by winds at any direction, but mostly those along the direction of the head. This

inflow is short lived and is usually dominated by the long term effects of the primary forcing at the mouth. The middle of the bay is essentially a mediation between the short effects of the lower primary forcing and the upper secondary forcing, wile retaining the long term effects of the primary forcing. While this point analysis is an effective qualitative tool, an EOF analysis was conducted to provide a quantitative spatial distribution of sub-tidal wind effects.

3.4 Correlation between EOFs and Wind Sub-tidal Effects

The first EOF represented 91% of the total variation in residual surface heights and corresponded highly with the EOF of Wang and Elliot in 1978. The spatial distribution shows that when the principle component (EOF time series) is positive, the whole bay is flooded as shown by the only positive values in the color bar: all sea surface heights in the bay are above normal. However, a gradient does exist. There is a low in the bottom of the bay and a piling up of water in the head of the bay as well as piling up of water on the western side of the bay. When the principle component is negative, the opposite distribution is produced, the whole bay is drained and a piling of water exists on the eastern and southern portions of the bay.

The second EOF represented 7% of the total variation in residual surface heights. Only a gradient extending from the head to the mouth exists across the bay. When the principle component (EOF time series) is positive, the only the bottom of the bay is flooded and the head is below normal, while the middle of the bay has little or no deviation. When the principle component is negative, the opposite occurs: a flooding of the head, draining of the mouth, and little deviation at the middle. Unlike the first EOF, the second did not show a non-local effect, wide-spread flooding or

draining across the bay; this difference will be further explained in the cross correlation diagrams.

The interpretation of the cross correlation diagrams between the wind and EOF principle component time series is extremely similar to the point residual analysis. Areas of high positive correlation represent a symmetric relationship between winds pointing in that direction and the positive EOF, i.e. winds in that direction cause a spatial pattern as in the positive EOF and winds opposite of that vector (the negative) cause the opposite spatial pattern, the negative EOF. Analysis of the EOF cross correlation diagrams ultimately supported the sub-tidal processes in the Chesapeake proposed by the point analysis.

In the point residual plots there is a short tem correlation at 90 and 270 degrees that differ between the northern plots and the southern plots. These local short term correlations are represented in the second EOF. The second EOF shows that north pointing winds recede incoming waters in the Delaware and push coastal waters in the mouth. Southern pointing winds do the opposite, pushing water out the mouth and into the head. The first EOF accounts for long term correlation found constant across the bay for winds along the direction of the head and the bay, but not for short term correlations along the North/South direction.

The difference between the first EOF and the second is that the first EOF, representing 91 percent of the total variance, shows the 'global' impact on the water levels in the bay due to winds in the direction of the head and the mouth. The second EOF, representing 6% of the total variance, shows the importance of wind direction concerning the head and mouth of the bay as

well, but represents the quick local effects. Essentially, the first EOF is a global or overall response to winds in the bay while the second emphasizes the differences between locations at the mouth of the bay and locations near the head.

Conclusion

Both the point and EOF correlation diagrams show that the winds are the dominant sub-tidal forcing in the Chesapeake Bay, inducing 97% of the residual surface height variation. In agreement with previous research, it was found that wind forcings induce two different categories of responses in surface height: a dominant, long-term, non-local response to fluctuations induced by the wind at the bay's mouth; and an immediate, local response to wind events. With the high spatial and temporal resolution of data obtained through a ROMs model, a more descript spatial distribution was obtained, furthering the understanding of the underlying physical oceanographic processes in response to the wind as well as serving as a better tool for tidal prediction across the Chesapeake Bay.

The highly resolute spatial distributions produced by the EOF can allow for the remote observation and prediction of sea surface heights in the Chesapeake. Given the wind speeds and directions of a meteorological event, the EOFs can be utilized to estimate sea surface heights across the bay from the wind and surface height values at least one location in the bay (i.e. a NOAA station); additional points, can further reduce uncertainty.

Predictions as well as the analysis completed in this study can be even further validated through the use of remote satellite data collection. The _____, with the ability to collect sea surface height and wind data, can provide actual observational data at the same resolution of the ROMs model. As shown through the historical progression of research on the sub-tidal variability of the Chesapeake, further data collection and resolution can only better understanding and prediction of tidal behavior.

Acknowledgements

This research was supported under

References

Barbosa, S. M., and M. E. Silva (2009). Low-frequency sea-level change in Chesapeake Bay: Changing seasonality and long-term trends, *Est. Coastal Shelf Sci.*, **83**, 30-38.

Boicourt, W. C. (2005), Physical response of Chesapeake Bay to hurricanes moving to the wrong side: Refining the forecasts, in *Hurricane Isabel in Perspective*, *CRC Publ. 05-160*, edited by K. G. Sellner, pp. 39-48, Chesapeake Res. Consortium, Edgewater, Md.

Bosley, K. T., and K. W. Hess (2001). Comparison of statistical and model-based hindcasts of subtidal water levels in Chesapeake Bay, *J. Geophys. Res.*, **106**, 16869-16885.

Chapman, D.C., Numerical treatment of cross-shelf open boundaries in a barotropic coastal ocean model, J. Phys. Oceanogr., 19, 384-391, 1985

Chuang, W. S., and W. C. Boicourt (1989). Resonant Seiche Motion in the Chesapeake Bay, *J. Geophys. Res.*, **94**, 2105-2110.

Flather, R.A., A tidal model of the northwest European continental shelf, Mem. Soc. R. Sci. Liege, 6, 141-164, 1976

Gong, W., J. Shen, K.H. Cho, an H. V. Wang (2009). A numerical model study of barotropic subtidal water exchange between estuary and subestuaries (tributaries) in the Chesapeake Bay during northeaster events, *Ocean Modelling*, **26**, 170-189.

Li, M., L. Zhong, and W. C. Boicourt (2005). Simulations of Chesapeake Bay estuary: Sensitivity to turbulence mixing parameterizations and comparison with observations, *J. Geophys. Res.*, **110**, C12004, doi:10.1029/2004JC002585.

Li, M., L. J. Zhong, W. C. Boicourt, S. Zhang, and D.-L. Zhuang (2006). Hurricane-induced storm surges, currents and destratification in a semi-enclosed bay, Geophys. Res. Letters, 33, L02604, doi:10.1029/2005GL024992.

Mukai, A.Y., J. J. Westerink, R. A. Luettich Jr., and D. Mark. Eastcoast 2001: a tidal constituent database for the western North Atlantic, Gulf of Mexico and Caribbean Sea. US Army Engineer Research and Development Center, Coastal and Hydraulics Laboratory, Technical Report, ERDC/CHL TR-02-24, 201p. September 2002

Shchepetkin, A. F., and J. C. McWilliams. The Regional Ocean Modeling System: A split-explicit, free-surface, topography following coordinates ocean model, Ocean Modelling, 9, 347-404, 2005

Shen, J., W. P. Gong, et al. (2006). Water level response to 1999 Hurricane Floyd in the Chesapeake Bay, *Cont. Shelf Res.*, **26**, 2484-2502.

Shen, J., H. Wang, M. Sisson, and W. Gong (2006). Storm tide simulation in the Chesapeake Bay using an unstructured grid model, *Est. Coastal Shelf Sci.*, **68**, 1-16.

Valle-Levinson, A., C. Reyes, and R. Sanay (2003). Effects of bathymetry, friction, and rotation on estuary-ocean exchange, *J. Phys. Oceanogr.*, **33**, 2375-2393.

Valle-Levinson, A., K. C. Wong, et al. (2001). Observations of the wind-induced exchange at the entrance to Chesapeake Bay, *J. Mar. Res.*, **59**, 391-416.

Wang, D. P. (1979). Wind-Driven Circulation in the Chesapeake-Bay, Winter 1975, *J. Phys. Oceanogr.*, **9**, 564-572.

Wang, D. P., and A. J. Elliott (1978). Non-Tidal Variability in Chesapeake Bay and Potomac River - Evidence for Nonlocal Forcing, *J. Phys. Oceanogr.*, **8**, 225-232.

Wong, K. C. and J. E. Moses-Hall (1998). On the relative importance of the remote and local wind effects to the subtidal variability in a coastal plain estuary, *J. Geophys. Res.*, **103**, 18393-18404.

Wong, K. C., and A. Valle-Levinson (2002). On the relative importance of the remote and local wind effects on the subtidal exchange at the entrance to the Chesapeake Bay, *J. Mar. Res.*, **60**, 477-498.

Xu, J., W. Long, L. W.J. Lanerolle, J. D. Wiggert, R. R. Hood, C. W. Brown, R. Murtugudde and T. F. Gross. Climate forcing and salinity variability in the Chesapeake Bay, USA. Estuarine and Coastal Shelf Science. (in prep.)

Zhong, L., M. Li, and M. G. G. Foreman (2008). Resonance and sea level variability in Chesapeake Bay, *Cont. Shelf Res.*, **28**, 2565-2573.

Tables

Table 1. Name, symbol and period of tidal constituents used in the harmonic analysis of the model's free surface [Source: U.S. National Oceanic and Atmospheric Administration (NOAA)].

No.	Species	Darwin Symbol	Period (hrs)	NOAA Order
1	Shallow water overtides of principal lunar	M_4	6.21030061	5
2	Shallow water overtides of principal lunar	M_6	4.140200402	7
3	Shallow water terdiurnal	MK_3	8.177139947	8
4	Shallow water overtides of principal solar	S_3	6.0	9
5	Shallow water quarter diurnal	MN_4	6.269173909	10
6	Shallow water overtides of principal solar	S_6	4.0	12
7	Lunar terdiurnal	M_3	8.280400814	32
8	Shallow water terdiurnal	2"MK_3	8.38630297	34
9	Shallow water eight diurnal	M_6	3.10515031	36
10	Shallow water quarter diurnal	MS_4	6.103339279	37
11	Principal lunar semidiurnal	M_2	12.42060122	1
12	Principal solar semidiurnal	S_2	12.0	2
13	Larger lunar elliptic semidiurnal	N_2	12.65834824	3
14	Larger lunar evectional	V_2	12.62600441	11
15	Variational	MU_2	12.87175763	13
16	Lunar elliptical semidiurnal second-order	2"N_2	12.90537448	14
17	Smaller lunar evectional	λ_2	12.22177415	16
18	Larger solar elliptic	T_2	12.0164492	27
19	Smaller solar elliptic	R_2	11.98359578	28
20	Shallow water semidiurnal	$2SM_2$	11.60695156	31
21	Smaller lunar elliptic semidiurnal	L_2	12.19162021	33
22	Lunisolar semidiurnal	K_2	11.96723479	35
23	Lunar diurnal	K_1	23.93446966	4
24	Lunar diurnal	O_1	25.81934166	6
25	Lunar diurnal	OO_1	22.3060742	15
26	Solar diurnal	S_1	24.0	17
27	Smaller lunar elliptic diurnal	M_1	24.83324836	18
28	Smaller lunar elliptic diurnal	J_1	23.09847677	19
29	Larger lunar evectional diurnal	ρ	26.7230533	25
30	Larger lunar elliptic diurnal	Q_1	26.86835667	26
31	Larger elliptic diurnal	$2Q_1$	28.00622255	29
32	Solar diurnal	P_1	24.06589016	30
33	Lunar monthly	M_m	661.3092049	20
34	Solar semiannual	S_{sa}	4382.905209	21
35	Solar annual	S_a	8765.82109	22
36	Lunisolar synodic fortnightly	M_{sf}	354.3670522	23
37	Lunisolar fortnightly	M_f	327.8589689	24

Figures

Figure 1. Map of ROMS model domain for the Chesapeake Bay model setup. The grid is shown superimposed onto the model's bathymetry field. The grid is composed of a total of 150 x 100 horizontal grid points with 20 levels in the vertical.

Figure 2. Sample time series of the sea-level variability from a selected grid point within the model domain. Harmonic analysis on the total simulated (free-surface) sea-level variability (blue curve) is used to calculate the tidal component (red curve) of the model's sea-level variability.

Figure 3. Map of the resulting a) co-range (m) and b) co-phase (units in hours) values for the ROMS predicted semidiurnal M_2 tide.

Figure 4. Sample time series of the residual sea-level variability (blue curve) from a selected point within the model domain. The residuals are obtained by subtracting the resulting tidal signal from the total sea-level variability signal and the sum of the two first EOFs time series (red curve).

Figure 5. [STILL NEEDED] A comparison between actual observed and model simulated subtidal/residual sea-level variability for 2006.

Figure 6. The resulting a) map and b) time series of the first mode of the Empirical Orthogonal Function (EOF) analysis of the residual sea-level variability from the CHESROMS model after removal of the tidal variability. This mode accounts for a total of 91.2% of the variance of the residual sea-level variation within the Bay.

Figure 7. The resulting a) map and b) time series of the second mode of the Empirical Orthogonal Function (EOF) analysis of the residual sea-level variability from the CHESROMS

model after removal of the tidal variability. This mode accounts for a total of 6.6% of the variance of the residual sea-level variation.

Figure 8. Cross-correlation between direction-specific components of the Bay's spatial-mean wind field and the first EOF mode of the subtidal/residual (model free surface minus tidal variability) sea-level variability.

Figure 9. Comparison between the time series of the first EOF and the magnitude of the wind component which demonstrated the highest cross-correlation with the first EOF.

Figure 10. Same as in Figure 8, but for the second EOF.

Figure 11. Same as in Figure 9, but for the second EOF.

Figure 12. Cross-correlation plots

Figure 13. Maps of the a) total, b) tidal, and c) subtidal/resdidual sea-level variance [m^2].

Figure 14. Maps of the percent of total sea-level variance [n.d.] from a) tide, b) sub-tidal/residual, and c) the sum of the tide and EOFs 1 and 2 components.

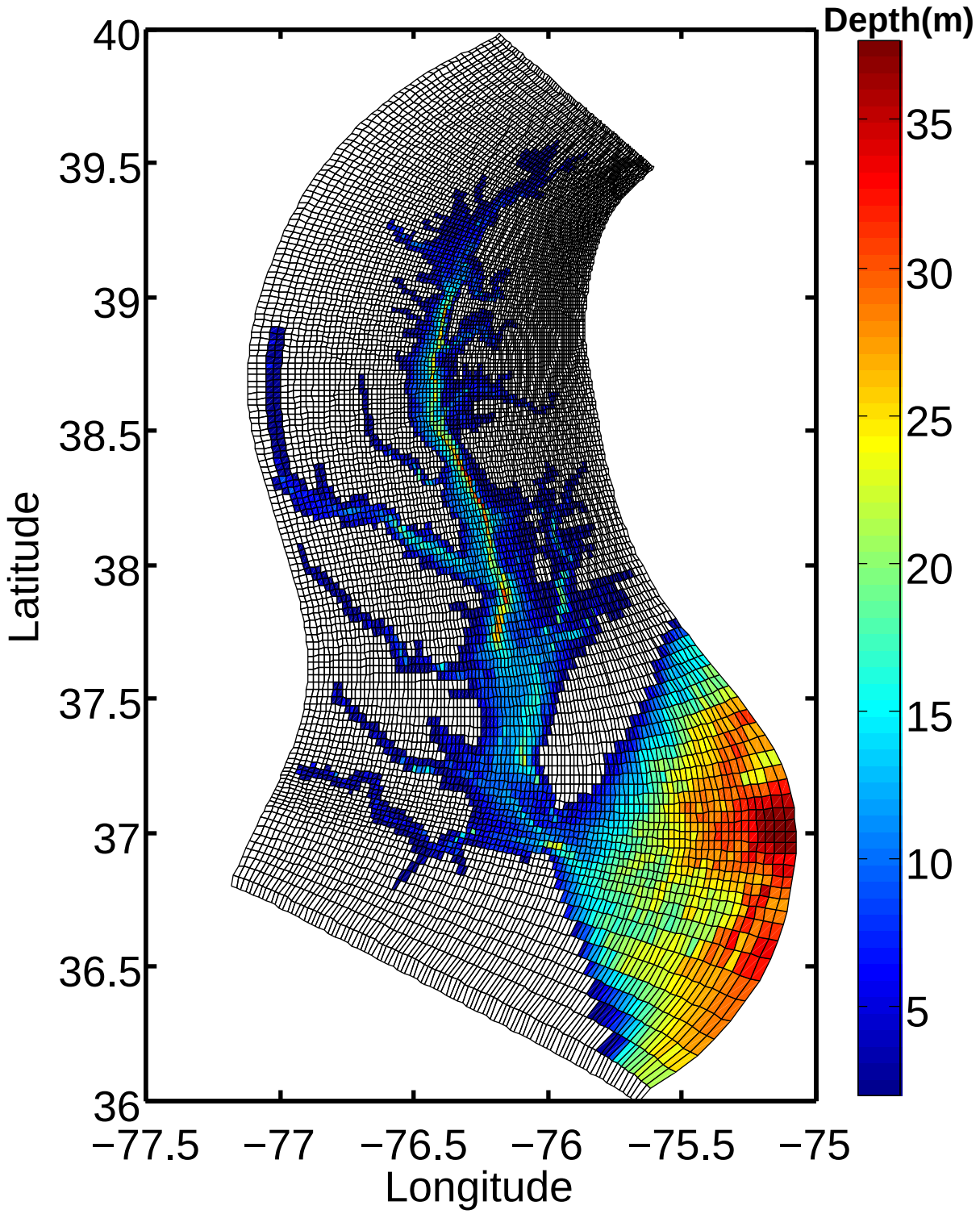
Depth(m)
35
30
25
20
15
10
5
40
39.5
39
38.5
38
37.5
37
36.5
36
Latitude
−77.5
−77
−76.5
−76
−75.5
−75
Longitude

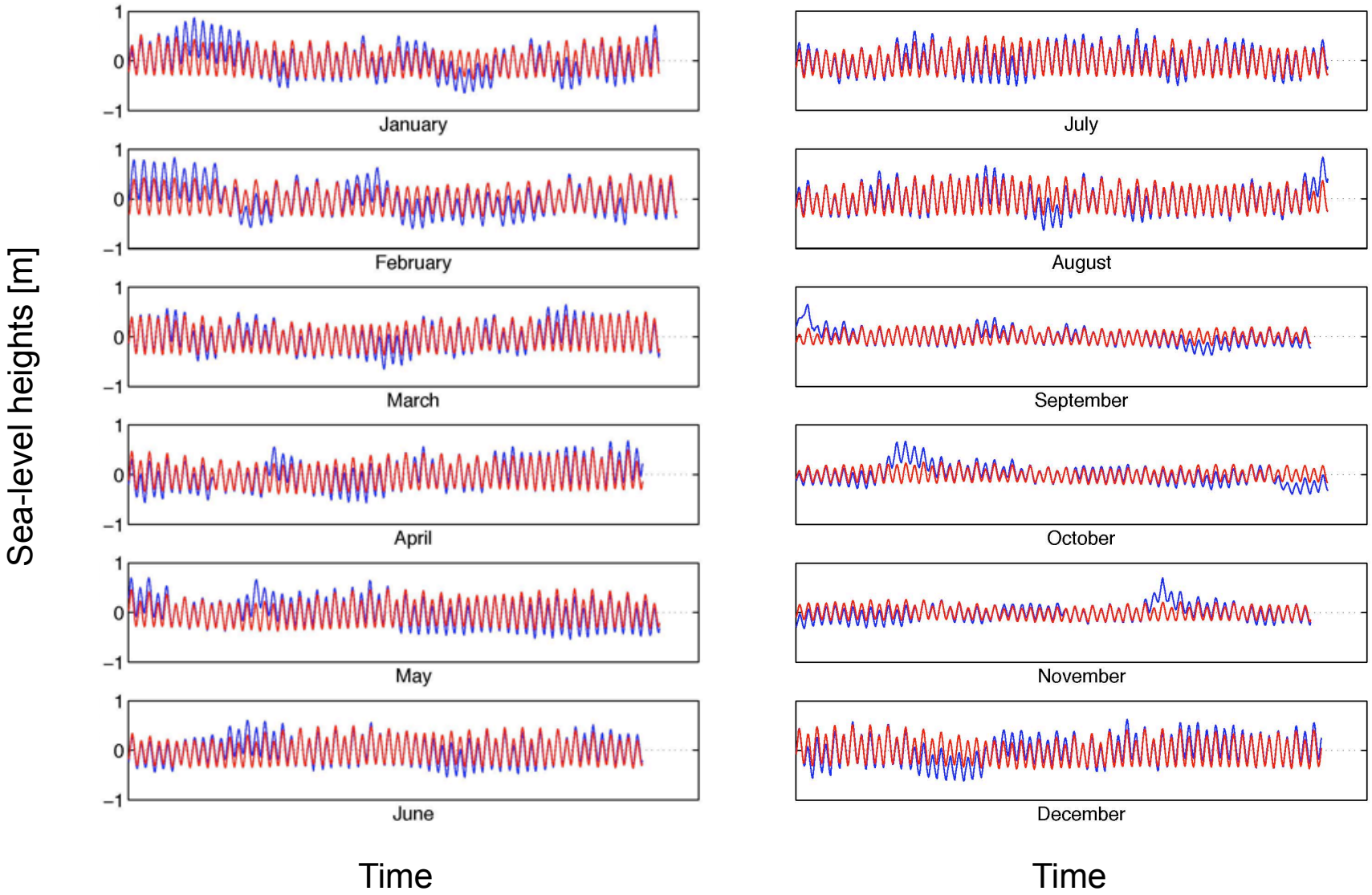
Sea-level heights [m]
1
0
−1
January
February
March
April
May
June
July
August
September
October
November
December
Time
Time

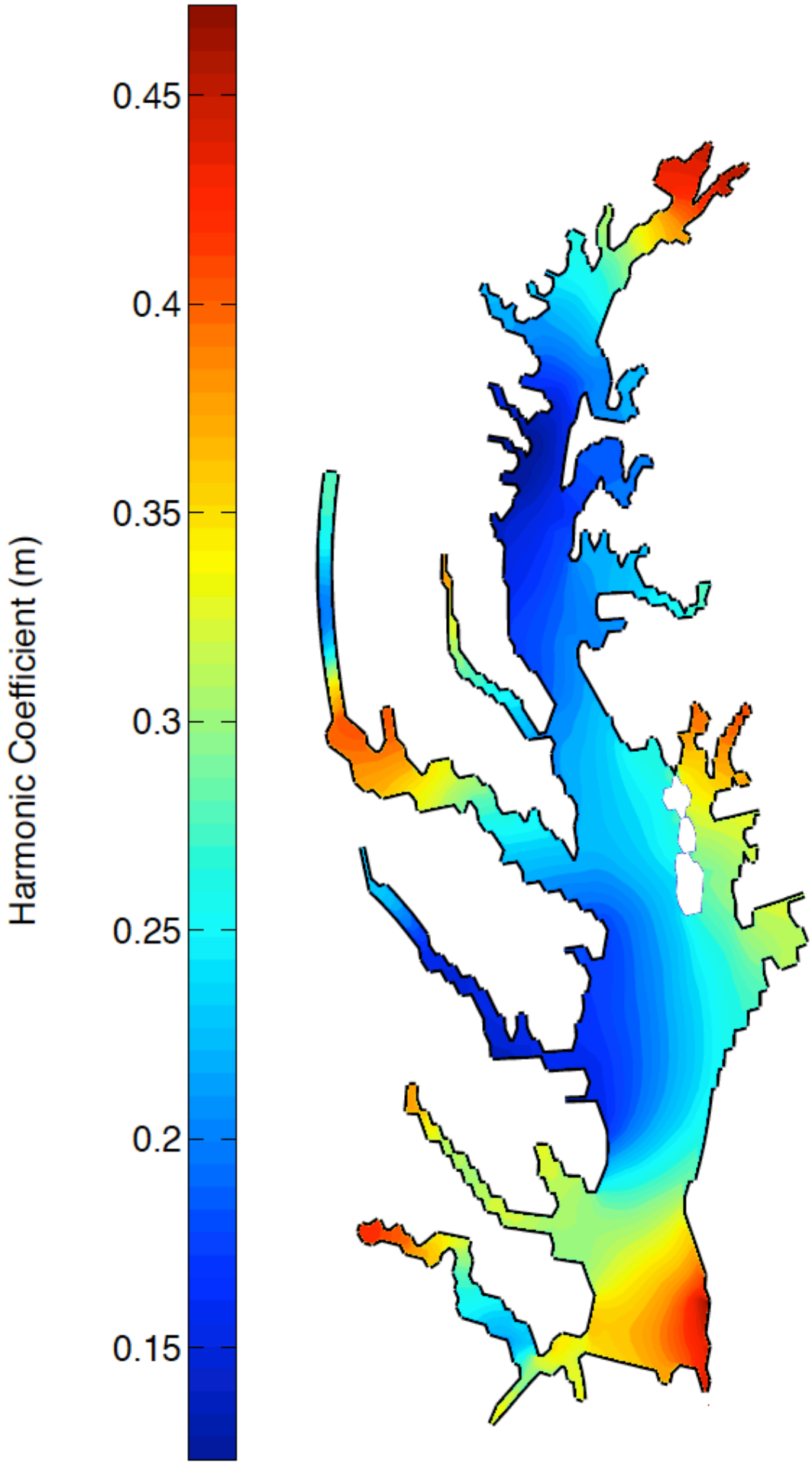
Harmonic Coefficient (m)
0.45
0.4
0.35
0.3
0.25
0.2
0.15

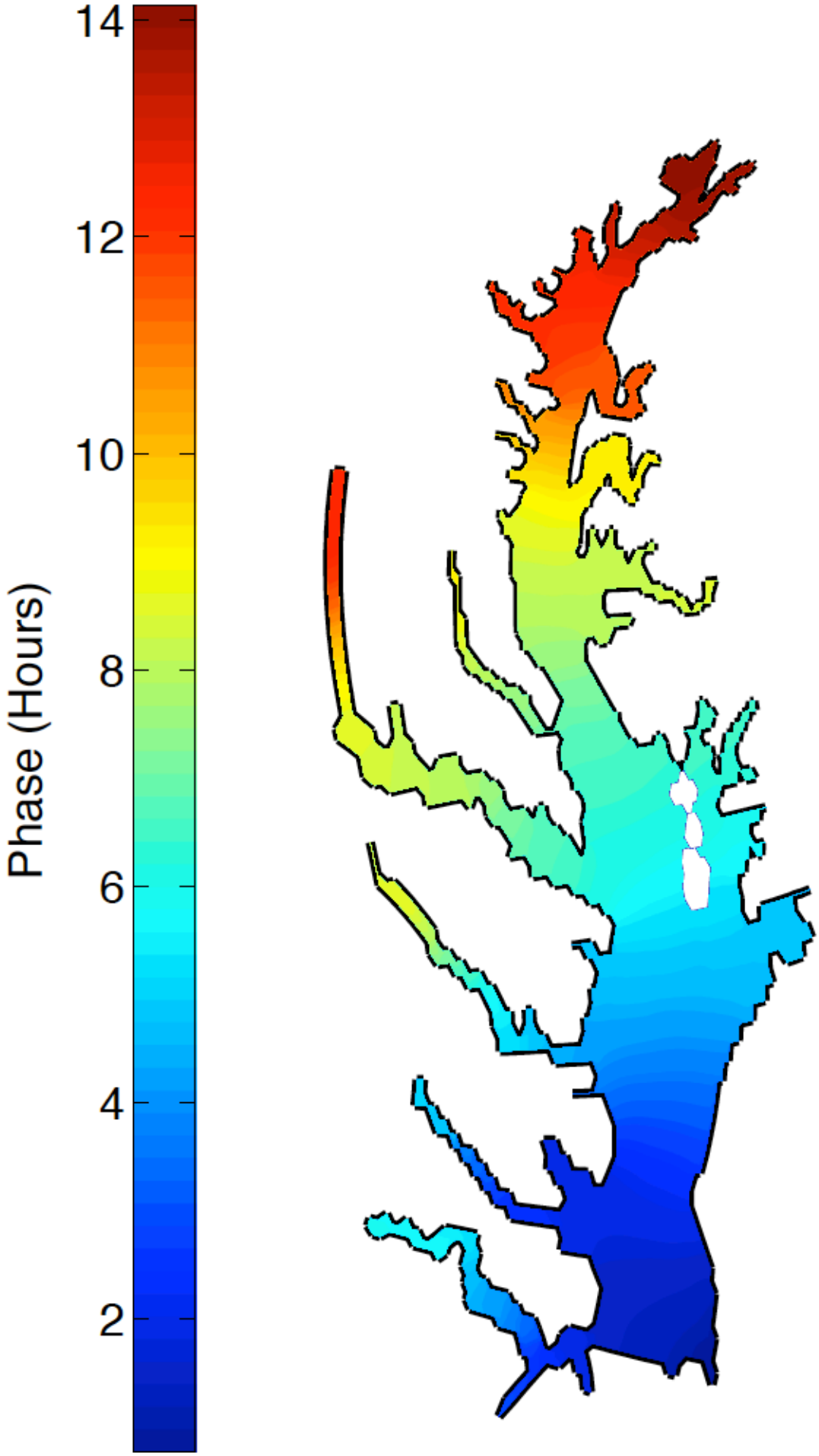
Phase (Hours)
14
12
10
8
6
4
2

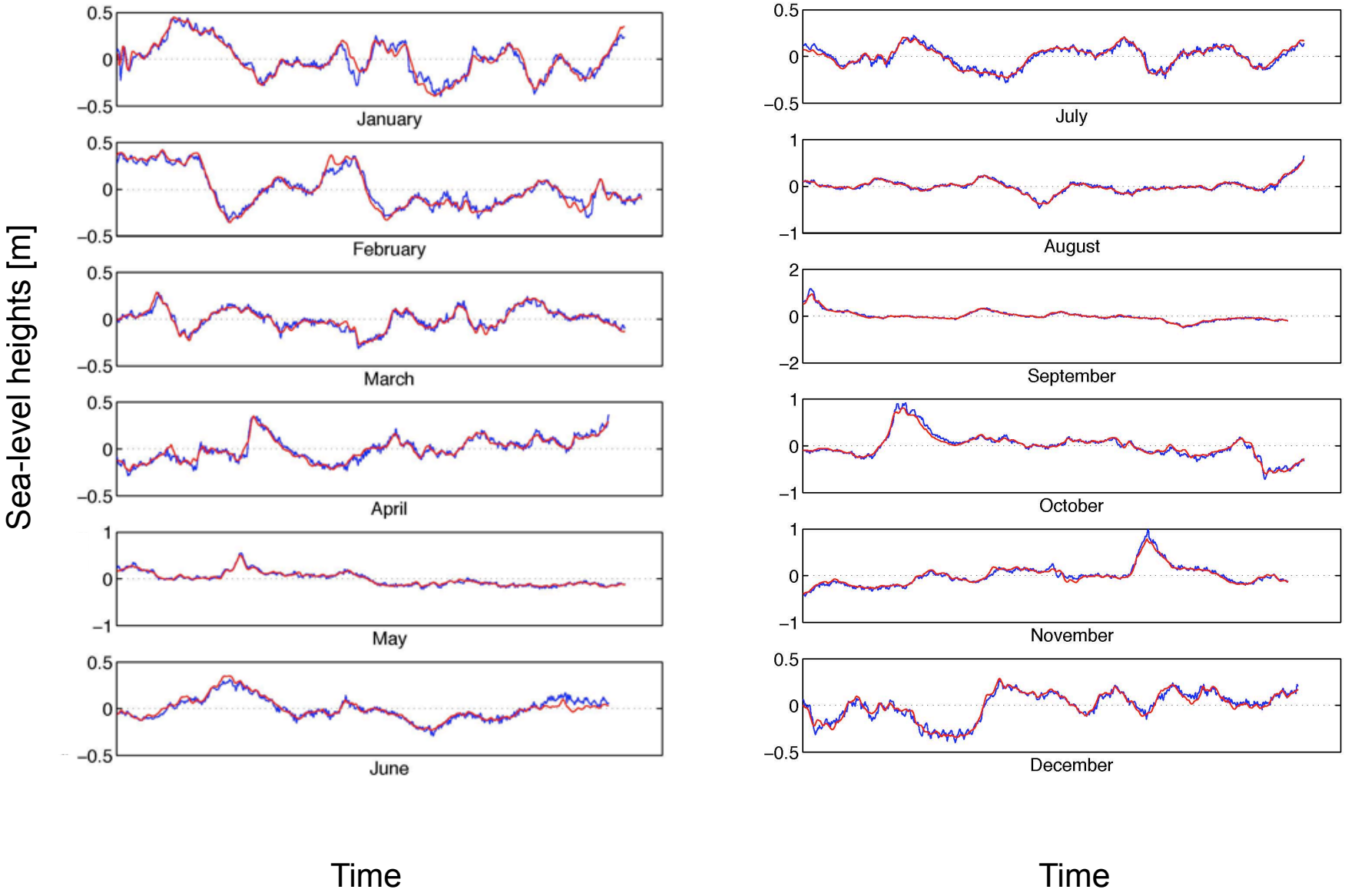
Sea-level heights [m]
January
February
March
April
May
June
July
August
September
October
November
December
Time
Time

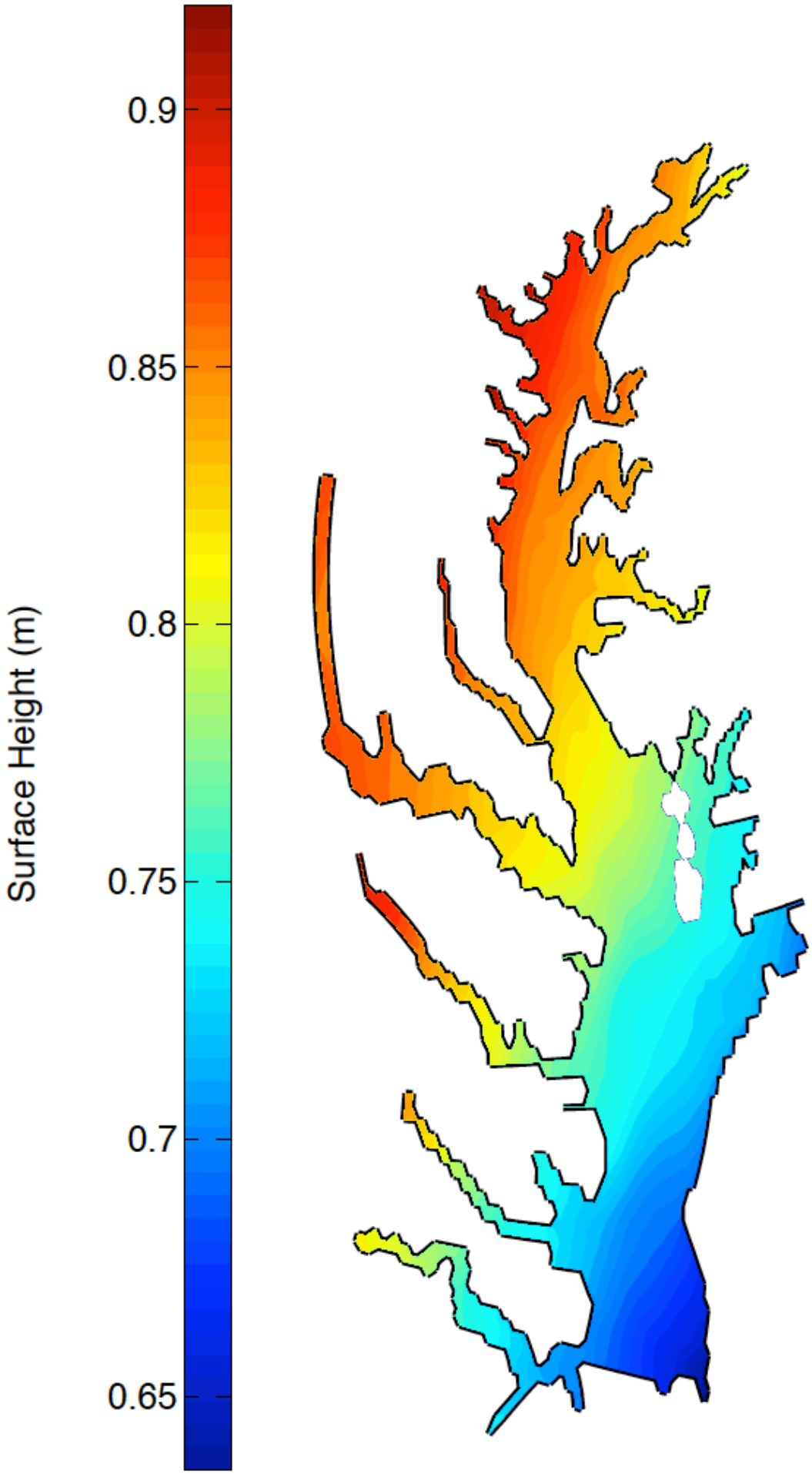
Surface Height (m)
0.9
0.85
0.8
0.75
0.7
0.65

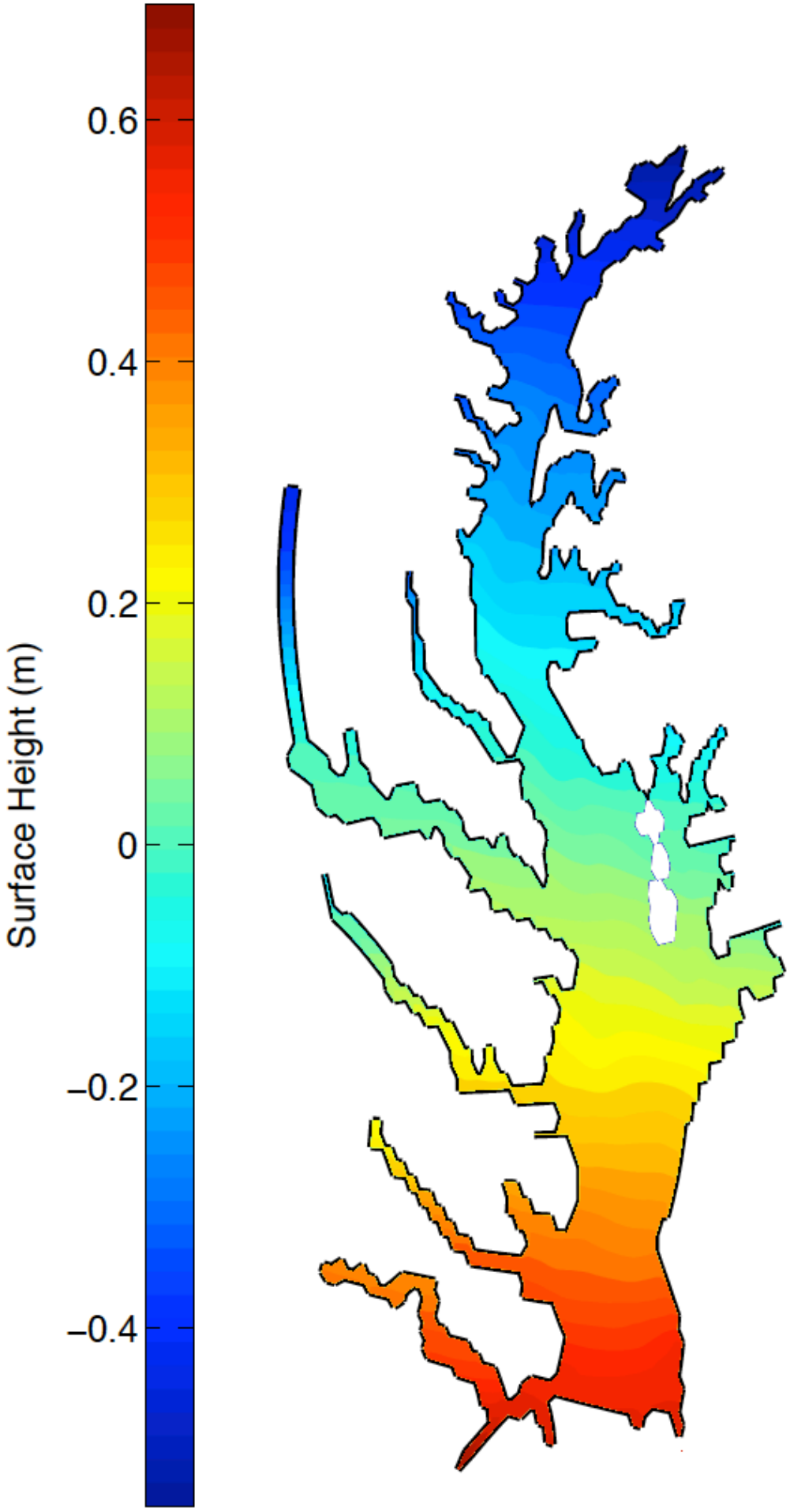
Surface Height (m)
0.6
0.4
0.2
0
−0.2
−0.4

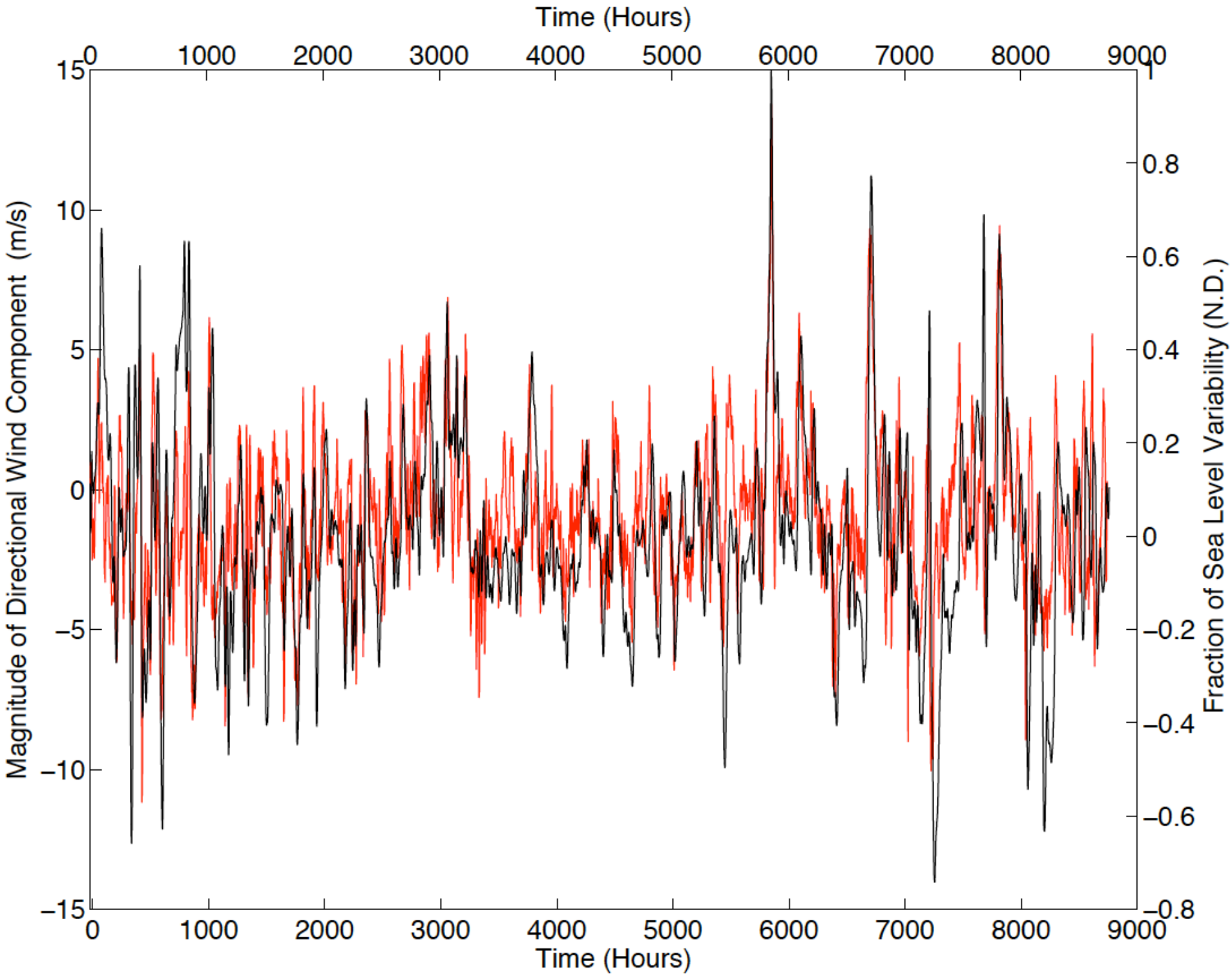
Time (Hours)
0
1000
2000
3000
4000
5000
6000
7000
8000
9000
15
10
5
0
−5
−10
−15
Magnitude of Directional Wind Component (m/s)
1
0.8
0.6
0.4
0.2
0
−0.2
−0.4
−0.6
−0.8
Fraction of Sea Level Variability (N.D.)
Time (Hours)

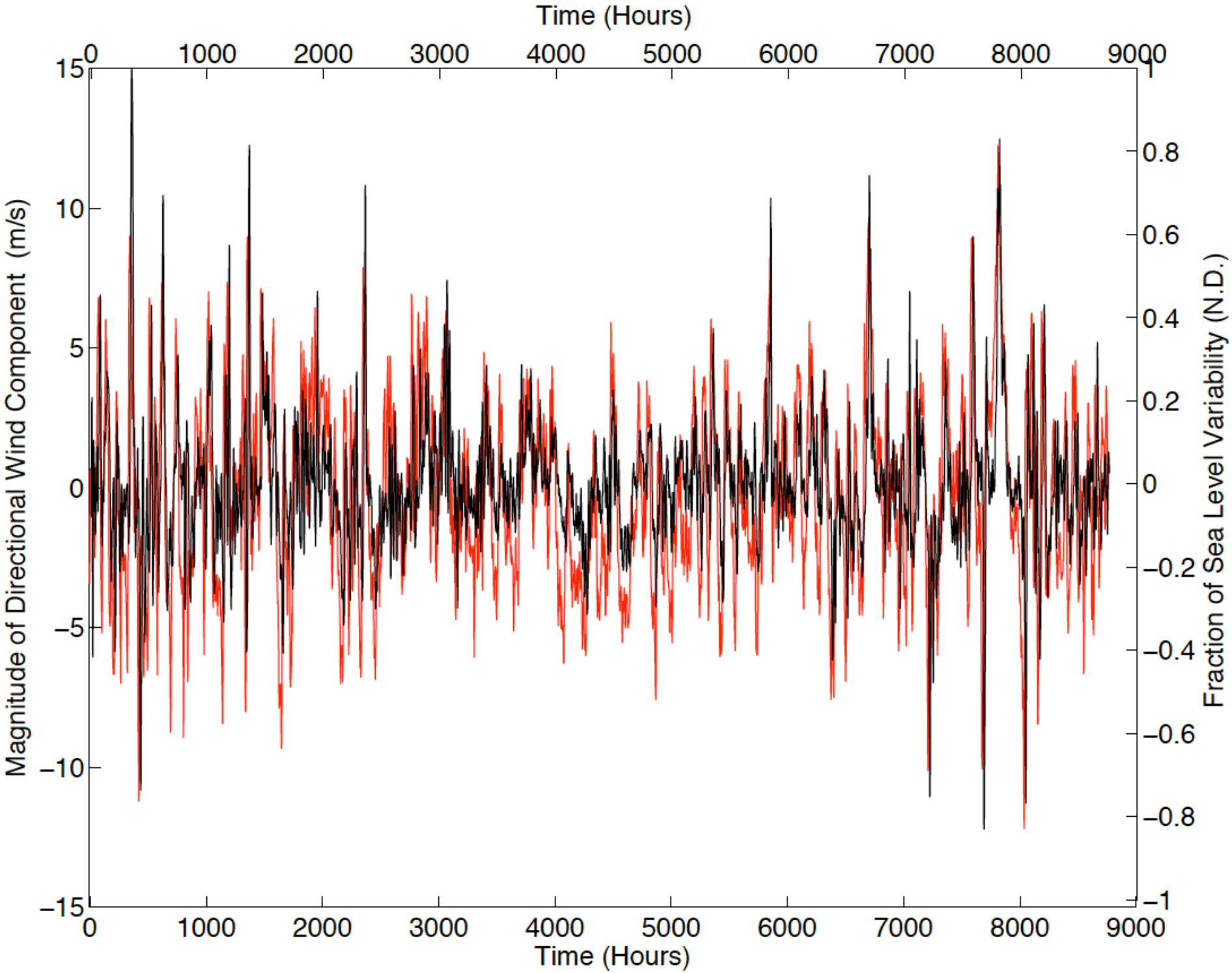
Time (Hours)
0
1000
2000
3000
4000
5000
6000
7000
8000
9000
15
10
5
0
−5
−10
−15
Magnitude of Directional Wind Component (m/s)
1
0.8
0.6
0.4
0.2
0
−0.2
−0.4
−0.6
−0.8
−1
Fraction of Sea Level Variability (N.D.)
Time (Hours)

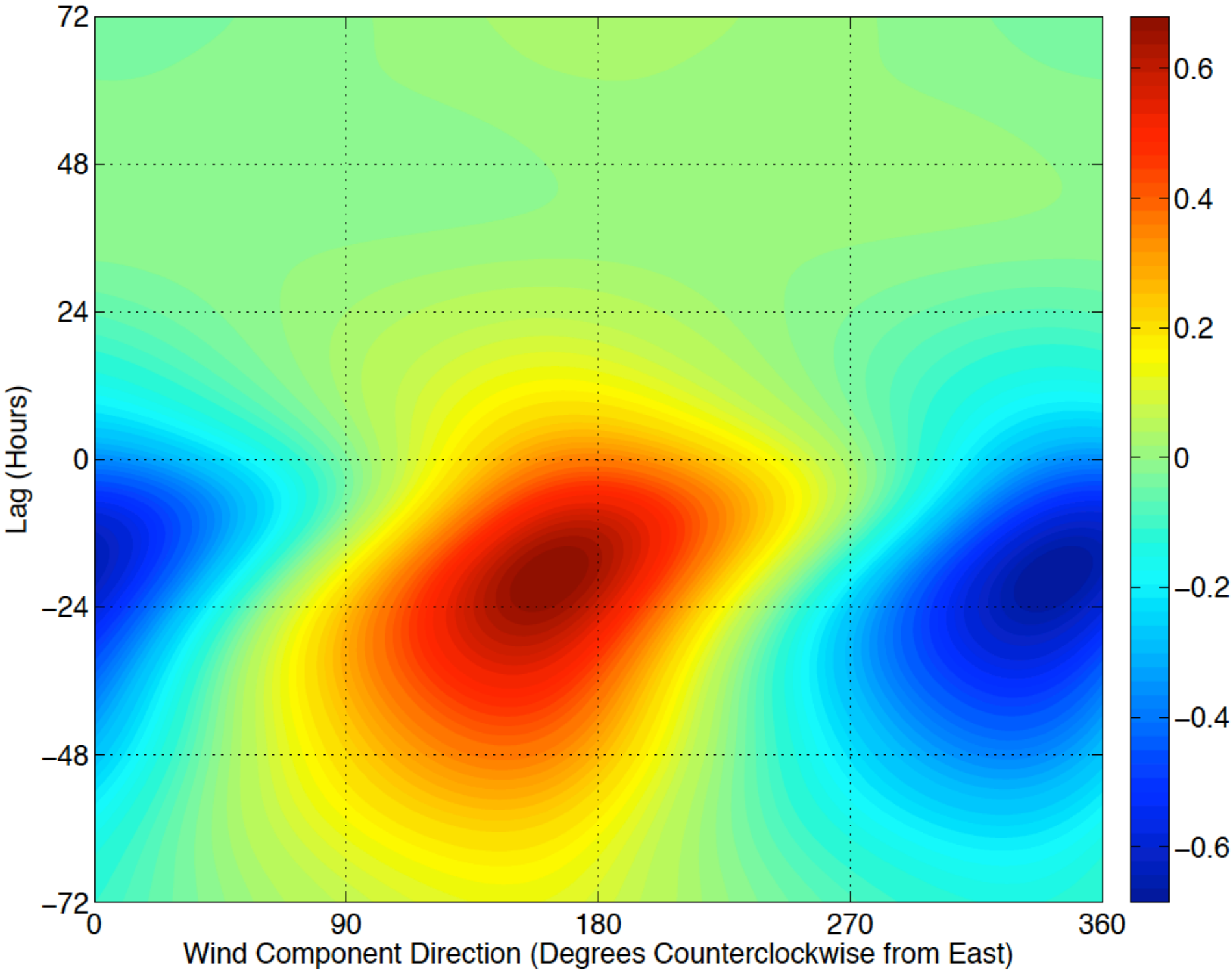
72
48
24
0
−24
−48
−72
Lag (Hours)
0
90
180
270
360
Wind Component Direction (Degrees Counterclockwise from East)
0.6
0.4
0.2
0
−0.2
−0.4
−0.6

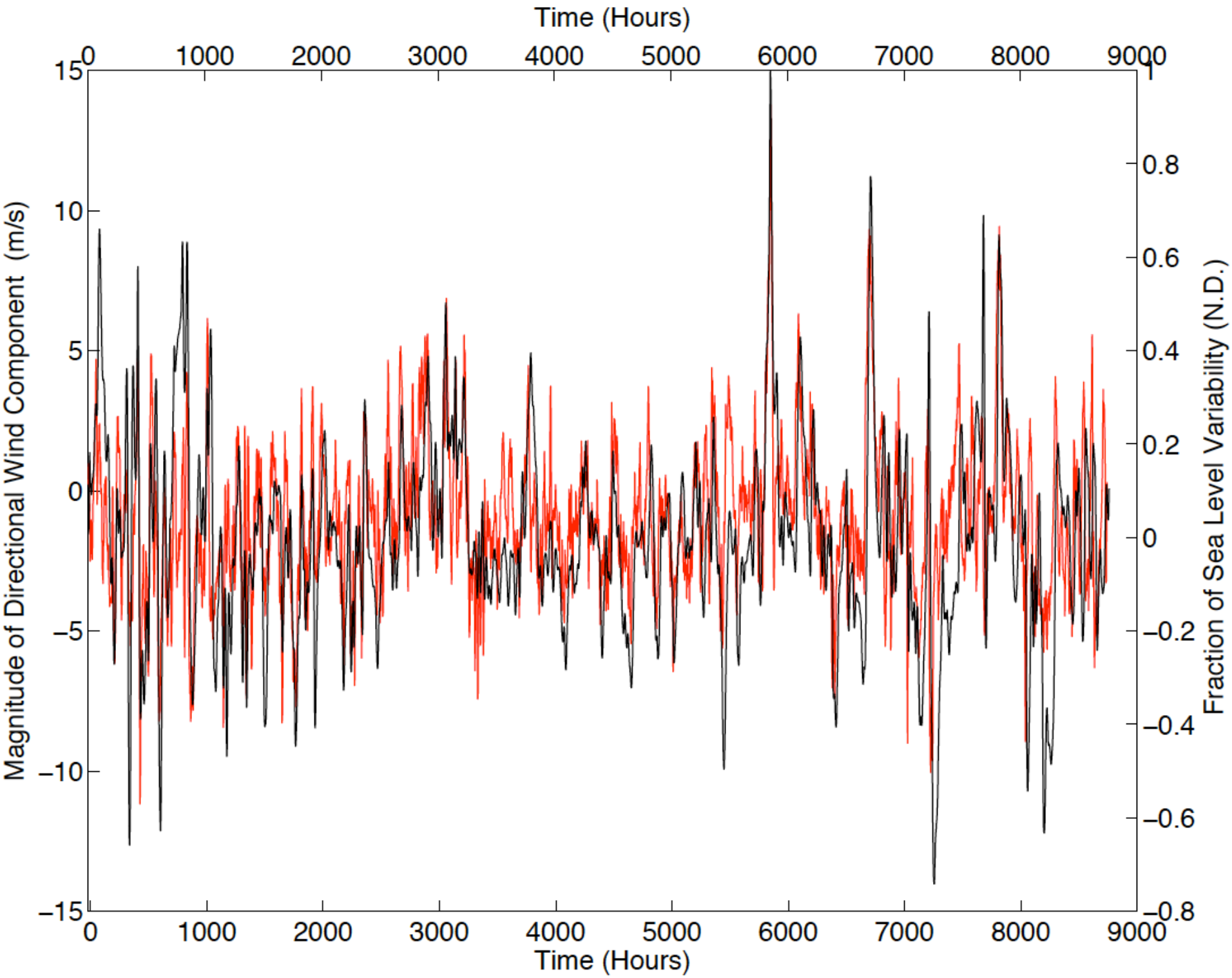
Time (Hours)
0
1000
2000
3000
4000
5000
6000
7000
8000
9000
15
10
5
0
−5
−10
−15
Magnitude of Directional Wind Component (m/s)
1
0.8
0.6
0.4
0.2
0
−0.2
−0.4
−0.6
−0.8
Fraction of Sea Level Variability (N.D.)
Time (Hours)

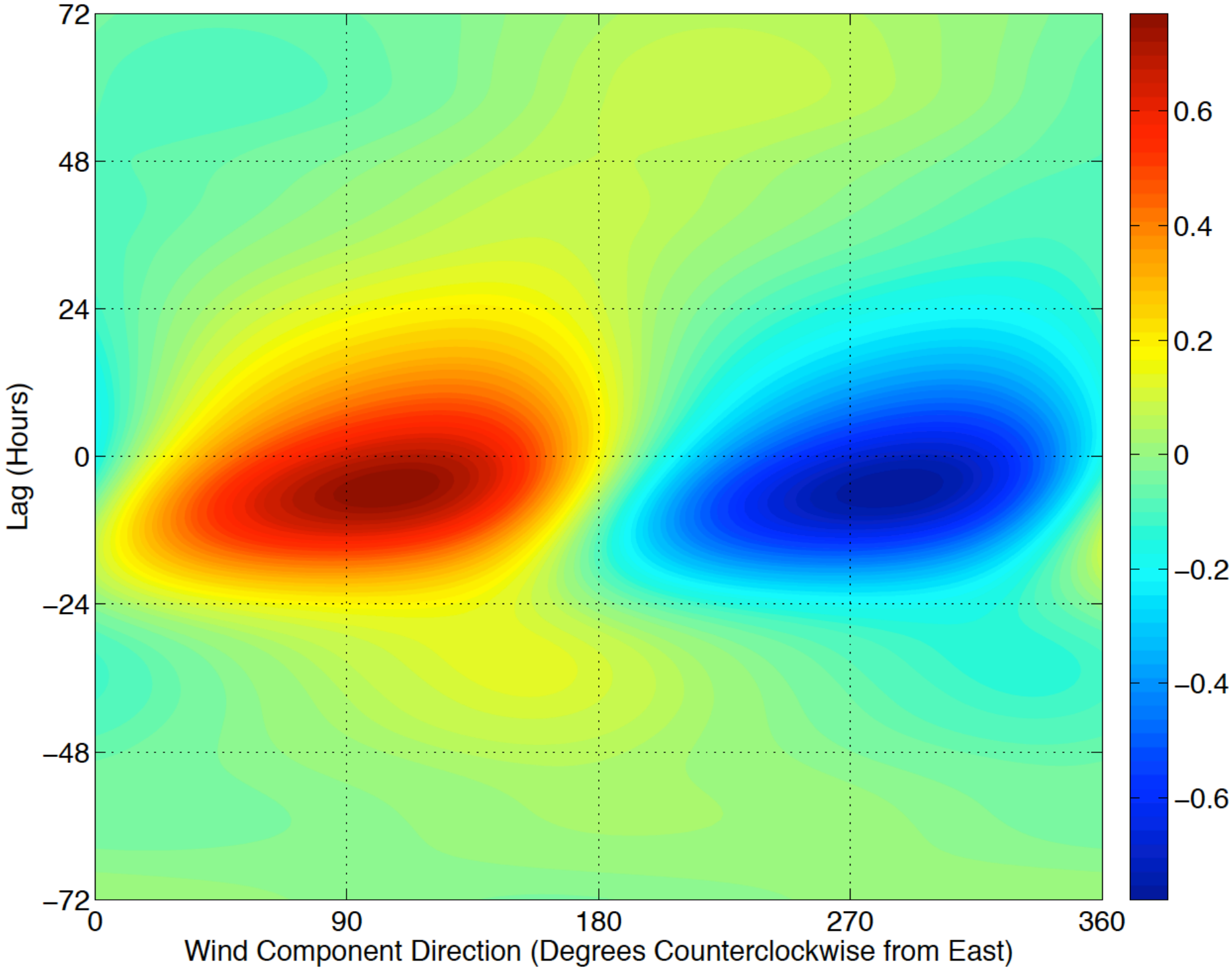
72
48
24
0
−24
−48
−72
Lag (Hours)
0
90
180
270
360
Wind Component Direction (Degrees Counterclockwise from East)
0.6
0.4
0.2
0
−0.2
−0.4
−0.6

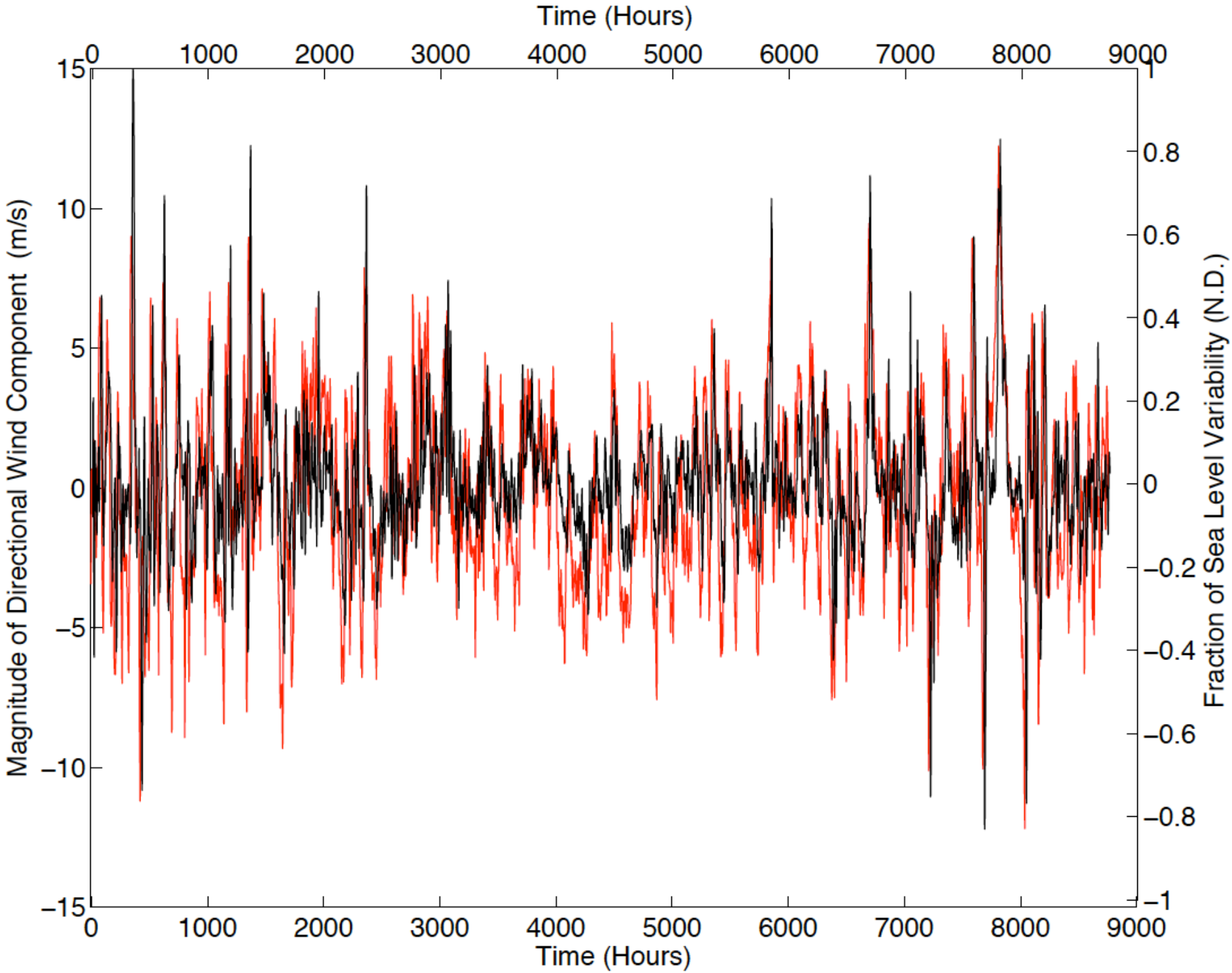
Time (Hours)
0
1000
2000
3000
4000
5000
6000
7000
8000
9000
15
10
5
0
−5
−10
−15
Magnitude of Directional Wind Component (m/s)
1
0.8
0.6
0.4
0.2
0
−0.2
−0.4
−0.6
−0.8
−1
Fraction of Sea Level Variability (N.D.)
Time (Hours)

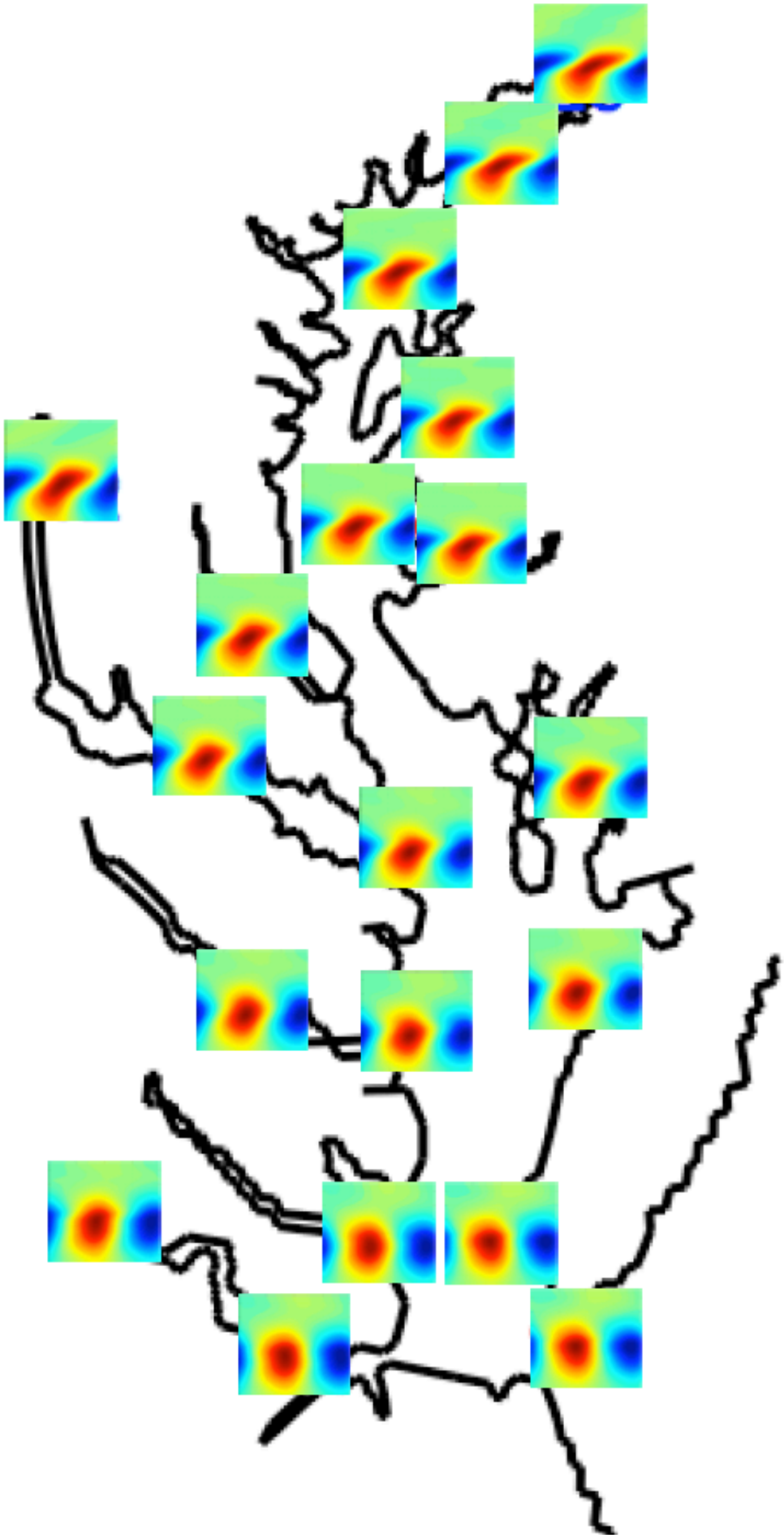

Total Sea-level Variance [m^2]

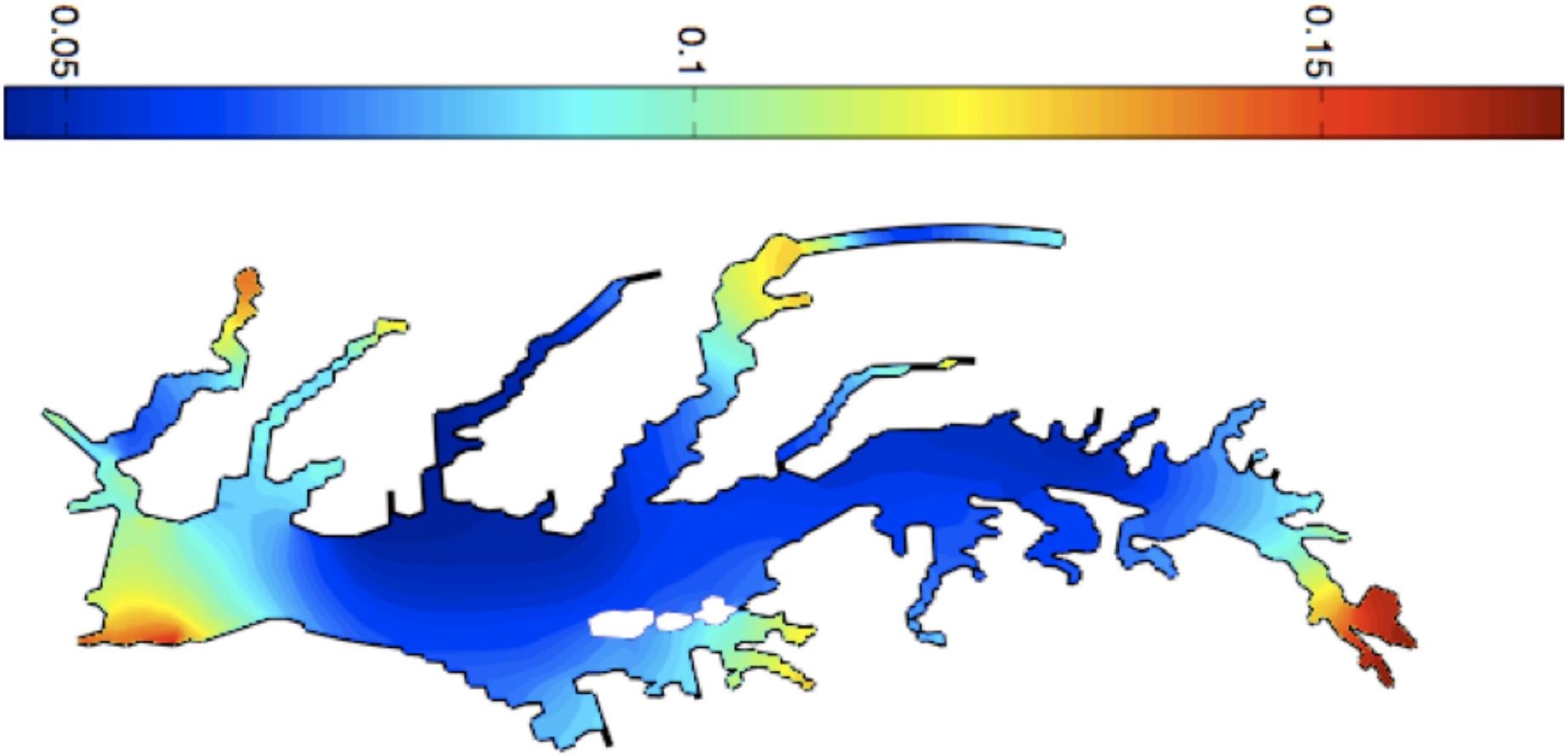

Sub-tidal/Residual Sea-level Variance [m^2]

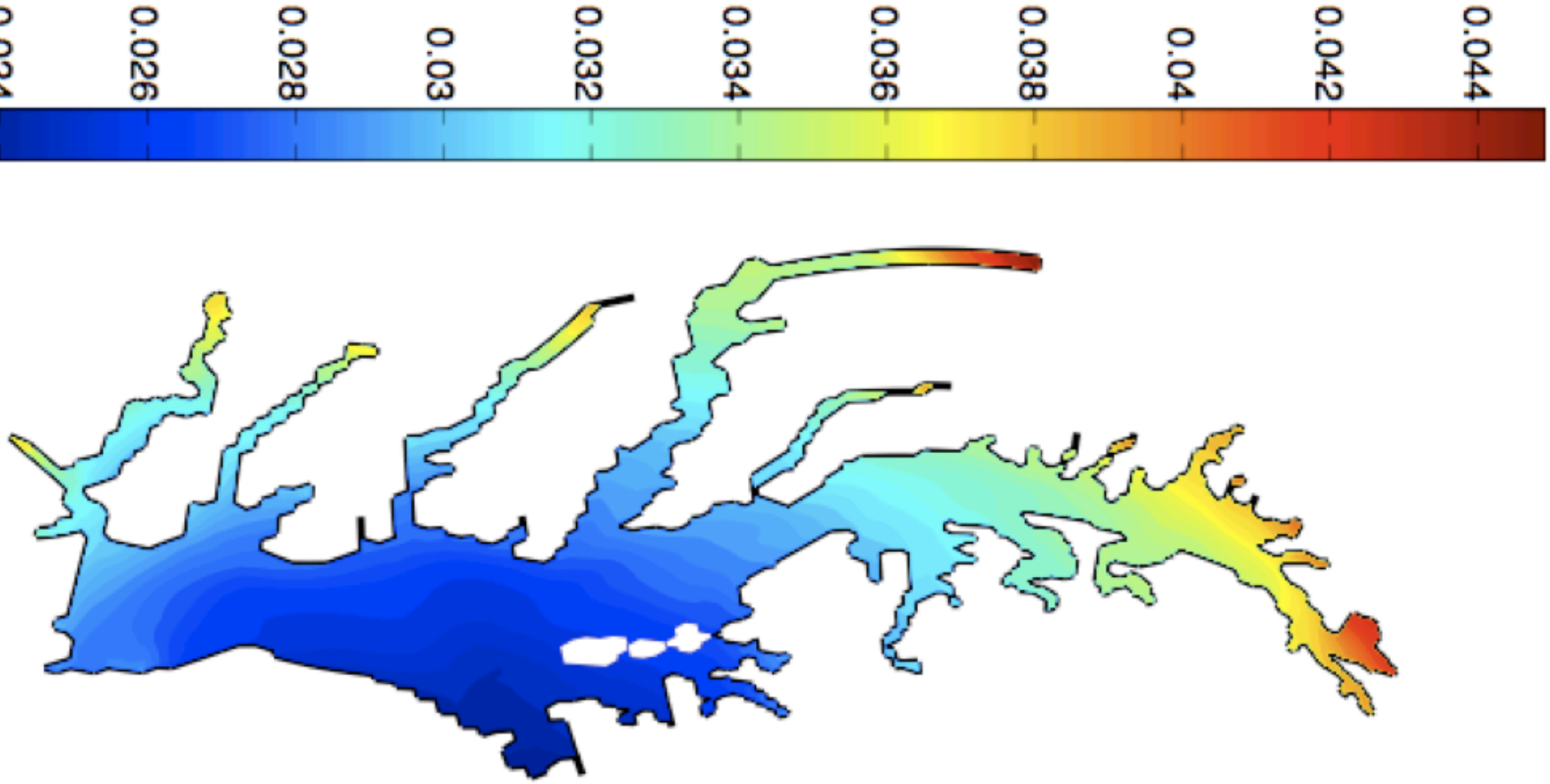

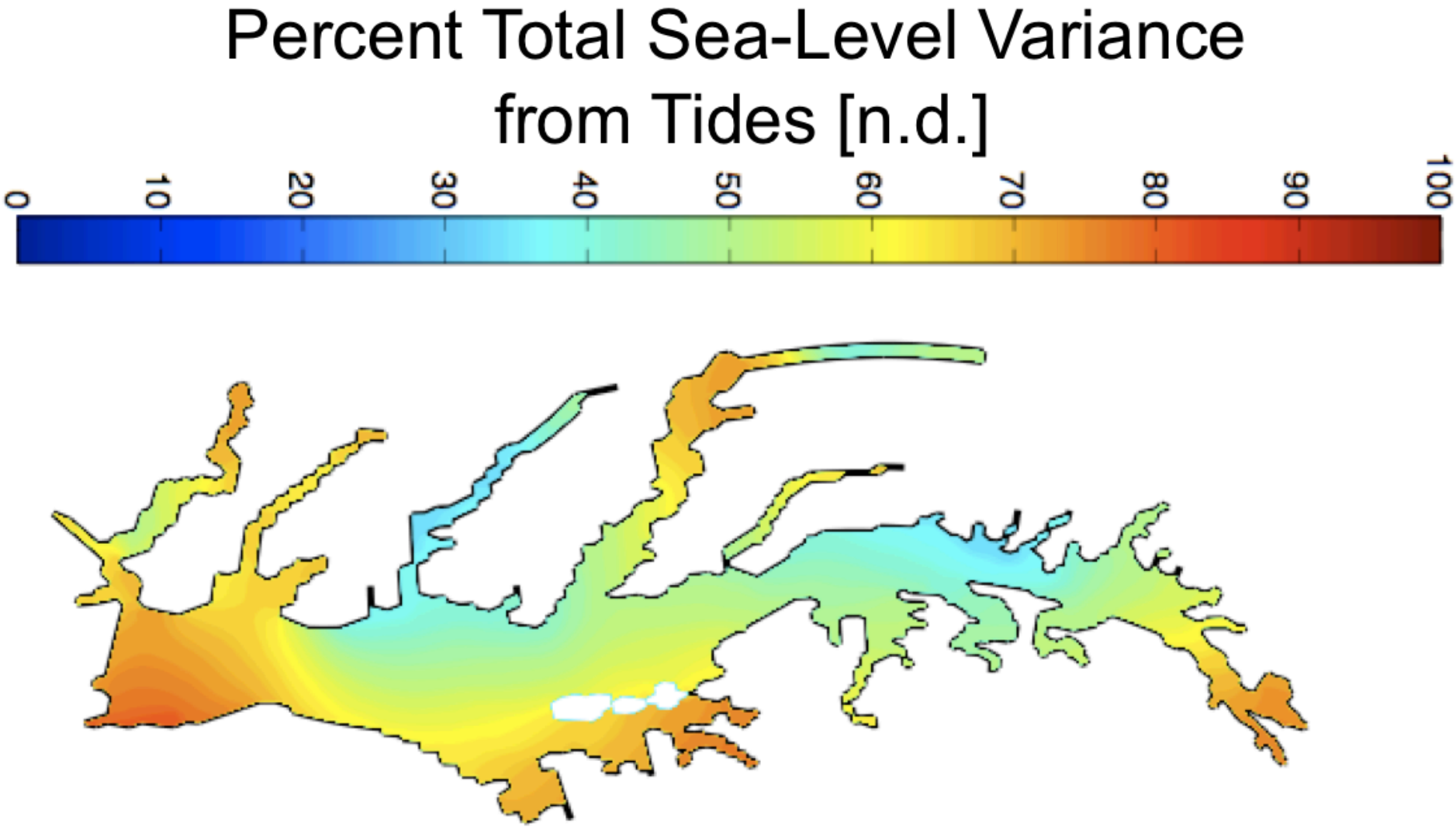
Percent Total Sea-Level Variance
from Tides [n.d.]
0
10
20
30
40
50
60
70
80
90
100

Percent Total Sea-level Variance from 1st EOF [n.d.]

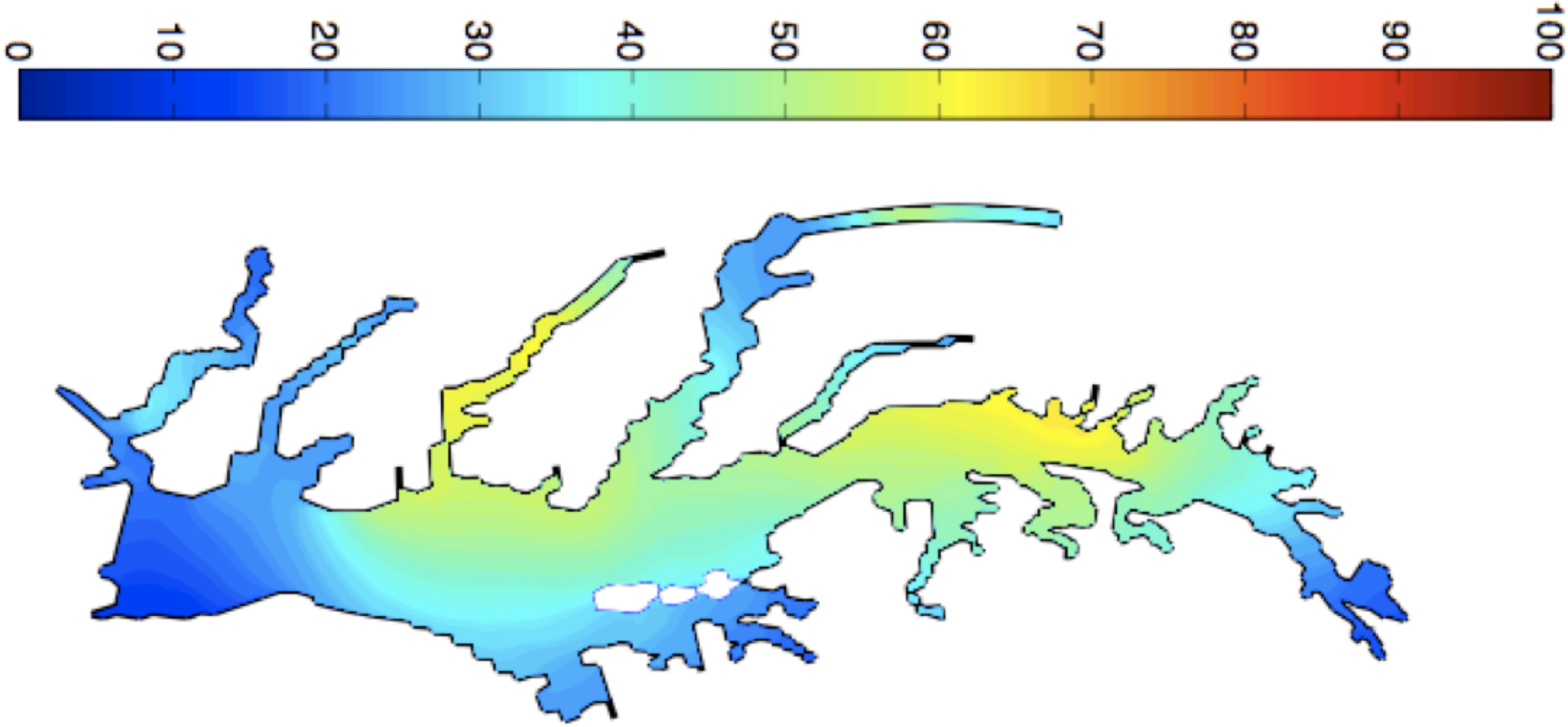
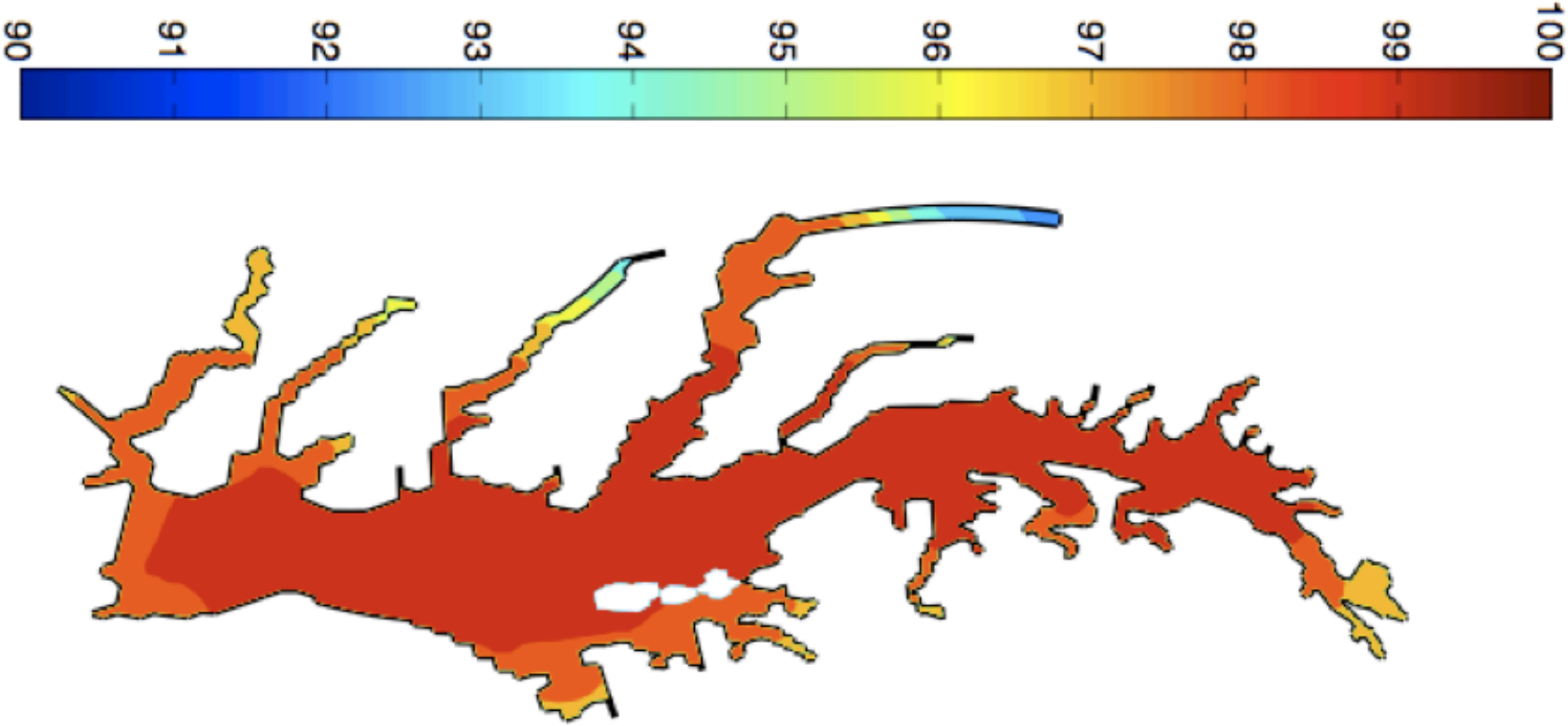
Percent Total Sea-level Variance From Tides + 1st and 2nd EOFs [n.d.]